
TECHNICAL REPORT 3275
May 2022

# Pseudobreathers in Saturable Klein-Gordon Equations

Richard C. Shockley

**NIWC Pacific**



Naval Information Warfare Center Pacific (NIWC Pacific)
San Diego, CA 92152-5001

This page is intentionally blank.

TECHNICAL REPORT 3275
May 2022

# Pseudobreathers in Saturable Klein-Gordon Equations

Richard C. Shockley

**NIWC Pacific**



**Administrative Notes:**
This report was approved through the Release of Scientific and Technical Information (RSTI) process in April 2022 and formally published in the Defense Technical Information Center (DTIC) in May 2022.



NIWC Pacific
San Diego, CA 92152-5001

**NIWC Pacific**
**San Diego, California 92152-5001**

A. D. Gainer, CAPT, USN
Commanding Officer

W. R. Bonwit
Executive Director

## ADMINISTRATIVE INFORMATION

The work described in this report was performed by the Advanced Systems branch of the Intelligence, Surveillance and Recon department, Naval Information Warfare Center Pacific (NIWC Pacific), San Diego, CA. The NIWC Pacific Naval Innovative Science and Engineering (NISE) Program provided funding for this Basic Applied Research project.

Released by
Thomas L. Jones, Branch Head
Advanced Systems

Under authority of
Michael McMillan, Department Head
Intelligence, Surveillance & Recon

## ACKNOWLEDGMENTS

We would like to thank Kelly Mckeever for her assistance in putting this report together and assisting in getting the report uploaded to RSTI to be published to DTIC.



Editor: RJP

# EXECUTIVE SUMMARY

## OBJECTIVE

The first objective of the work reported here was to determine, by numerical simulations, whether self-localized, nonlinear waves akin to "breathers" exist for a certain subset of "saturable" Klein-Gordon (KG) equations. (Terms are explained in Section 1.) Breatherlike waves do arise in these equations, so the second objective was to study their decay and their interaction in collisions. Saturable KG equations govern diverse physical systems. The simplest example is a taut string subject to an external restoring force transverse to its length at rest. This could be the force of gravity on a string sliding on the wall of a V-shaped trough with a rounded, parabolic bottom. The restoring force is proportional to the displacement for small displacements from equilibrium and monotonically approaches a constant value asymptotically, or "saturates," for large displacements.

## RESULTS

Analytic (infinitely differentiable) functions were developed for six saturable restoring forces as described above, along with their potential energy functions, equivalent to the cross-sectional shapes of a trough as mentioned above. Simulations have shown that the corresponding KG equations all have breatherlike waves. We call these blobs "pseudobreathers." These waves seem to have gone unreported previously, despite the extremely extensive literature on breathers. An infinitude of like KG equations must exist with similar pseudobreathers. They are stable, meaning they radiate only a tiny fraction of their energy over thousands of cycles. They attract or repel slightly in collisions, and emerge from collisions nearly unchanged in shape, despite being nonlinear. They are like beads sliding on a wire, and could potentially act as bits or general information packets in nanomechanical memory or signal-processing devices, perhaps using graphene nanotubes, or be used for quantum computation. Several examples are given of extremely simple electrostatic, gravitational, magnetostatic, and mechanical systems obeying saturable KG equations. The methods for initializing and simulating pseudobreathers are presented.

## RECOMMENDATIONS

Since we have no theory for the decay or collision of the pseudobreathers treated here, theoretical development appears the most important and interesting extension of this work. Simulations should provide deeper insight into the dynamics of collisions and show whether pseudobreathers settle into more stable states after radiating some amount of energy or form bound states like molecules. They could also explore the possible conversion of a narrowband pulse into discrete localized pseudobreathers or the reverse by having either reflect from or be transmitted through a longitudinal inhomogeneity, equivalent to a constriction in the troughs mentioned above. Generalizing the one-dimensional finite-difference simulation equations to two spatial dimensions is also of interest, as is the question of how our results might bear on quantum computation.

This page is intentionally blank.

# CONTENTS



# Figures

# 1. INTRODUCTION: NONLINEAR WAVES, SOLITONS, AND BREATHERS

This report begins by discussing the difference between linear and nonlinear waves in ordinary language. This is background for readers unfamiliar with linear wave theory or new to nonlinear waves. It is assumed that the reader has mathematical skills at the undergraduate level in science and engineering, but mathematical results are often restated in ordinary terms to give a nontechnical reader a sense of the aesthetic appeal of the particular nonlinear waves addressed here. We call these waves "pseudobreathers." They are self-localized oscillations resembling standing waves, such as the lowest mode of vibration of a taut string with fixed end-points. They are interesting because they behave like particles, but not like either classical "Newtonian" particles nor quantum mechanical particles.

Solitons and breathers are the two kinds of nonlinear waves that have drawn greatest attention. These are described after the general introduction to linear and nonlinear waves along with remarks on their history. Background is then given on the work to be presented here, the main results are described, and the sections to follow are outlined. The best introduction to nonlinear waves could be the book by G. B. Whitham [1], but there might be over 100 books on solitons in print. The excellent undergraduate text by Resnick and Halliday [2] is recommended for explaining terms in standard physics that are mentioned in passing.

The derivations in this report use only basic calculus and complex exponentials. Moreover, the essential self-trapping property of the pseudobreathers discussed here is understandable on intutive grounds (see Section 2.4). We lack analytic theory for their decay and dynamics in collisions. This is a report on ongoing research aiming to show results to date. References are not cited as extensively as would be appropriate for a paper in a peer-review journal.

Solitons, true breathers, and pseudobreathers have been studied intensively for over fifty years, yet the pseudobreathers that arise in saturable Klein-Gordon (KG) equations treated here seem to have escaped systematic study. This is striking. Saturable nonlinear systems have indeed been studied theoretically and experimentally, but most such work has addressed other classes of nonlinear wave equations. The closest nonlinear wave equation to those treated here is the sine-Gordon equation. This equation possesses true solitons and breathers. It and modified versions of it have received much attention. The general behavior of pseudobreathers in saturable KG equations ought to be of fundamental interest. This is not merely on mathematical grounds, but because of possible applications of pseudobreathers, and specifically those using nanoscale devices that might advance technology beyond the Silicon Age.

Sound waves, light, and ripples on a pond's surface, in ordinary experience, are called "linear." This means that they pass cleanly through each other. When two beams of sound intersect, the deviation from the ambient acoustic pressure is just the sum of the acoustic pressure of each separate beam. When beams of light intersect, the electric and magnetic fields are the sum of the fields of each separate beam. When ripples from two ducks on a pond intersect, the height of the water above or below its normal level is the sum of that from each duck. Linear waves simply stand on each other's shoulders when they meet. This is known as the "principle of linear superposition."

Waves obeying the principle of linear superposition do not exchange energy or momentum. They do not push on each other nor change each other's direction. After having met, they go on their way as if the other wave were never there. Also, in daily experience, when the intensity of the light incident on a pane of glass is doubled, no other changes being made, the sole effect is that the intensity of the light transmitted through the pane doubles. The transmitted intensity is directly proportional to the incident intensity.

Linear superposition is of great importance in simplifying problems. We treat a wave as a sum of independent sinusoidal oscillations like the "pure" tone emitted by a tuning fork. This is known as

"Fourier" or "spectral" analysis. It could be the most widely used analytic method in science and engineering. To solve a problem involving transient waveforms, we consider what happens with one wave at one frequency, a far simpler problem, and then compute the weighted sum or integral over all the frequencies that make up the transient waveform of interest.

Linear superposition fails eventually as the intensity of sound, light, or other kinds of waves increases. Shock waves, for example, are basically different from the acoustic waves in daily life. A shock wave travels faster than the usual speed of sound. In the familiar situations, the speed of sound is very nearly a fixed number, whether in air, water, steel, or glass. It might vary by a few percent depending on the circumstances. In seawater, it varies slightly with pressure, salinity, and temperature over a range of about $5\%$ around $1480\,\mathrm{m/s}$. The speed of sound is dictated by the compressibility, or equivalently, the rigidity or the stiffness of a medium, not its density. In daily experience, the speed of sound does not depend on its intensity. The same holds true for light.

A shock wave, on the other hand, travels faster with increasing intensity. Similarly, an intense laser beam can heat the air, a pane of glass, a crystal, or liquid, or produce other effects that change the beam as it travels through the medium. The change is self-induced. For example, a strong enough red laser beam can generate an accompanying beam of blue light on passing through certain kinds of crystals.

These and other amplitude-dependent effects, such as the crackling heard from an overdriven microphone or loudspeaker, are called "nonlinear." The qualitative behavior of nonlinear waves depends on their intensity, or equivalently, on the strength of the acoustic, electromagnetic, or other fields involved. Nonlinear effects are undesirable in some instances and desirable in others. In general, nonlinear behavior is harder to analyze than linear behavior. One usually settles for an approximate theory.

An example of a nonlinear optical effect is self-focusing [3]. Self-focusing may occur for several reasons. One of these is molecular reorientation, which occurs in $\mathrm{CS_2}$ (carbon disulfide), a colorless, odorless liquid at room temperature with prolate spheroidal (football-shaped) molecules. Random thermal jiggling makes the long axis of each molecule equally likely to point in any given direction, so $\mathrm{CS_2}$ is ordinarily isotropic.

A linearly polarized, planewave laser beam causes $\mathrm{CS_2}$ molecules to align to some degree with their long, or "easy," axis of polarization parallel to the electric field. This increases the polarizability of the medium, and most strongly along the axis of the beam. The larger polarizability in turn increases the index of refraction and reduces the phase velocity. The phase velocity means the speed of phase-fronts. One can pictures crests or troughs of ocean waves or the ranks of a marching band. By definition, the phase-velocity is equal to the speed of light in vacuum divided by the index of refraction.

The wavefronts are therefore delayed near the axis of the beam relative to the wings or tails of the beam. The result is the same kind of wavefront curvature as is caused by a focusing lens, which is thick in the middle and tapers at the edges. For a sufficiently intense beam, the beam tends to focus instead of expanding owing to diffraction as it would otherwise. Self-focusing can damage a medium. It limits the power of intense lasers in glass optics in laser-induced fusion experiments. In glasses, to a first approximation, the change in the index of refraction is proportional to the beam's intensity, which is known as the "Kerr effect."

The opposite effect occurs in thermal blooming. This occurs when a strong microwave beam in the air heats the air, again most strongly along the beam's axis. The hotter air expands, reducing its density and increasing the phase velocity near the beam's axis. This causes a curvature of the wavefronts like that produced by a diverging lens. The beam naturally diverges or "blooms." Hence intense microwave beams are impractical as long-range weapons in the earth's atmosphere.

Solitons and breathers are two kinds of nonlinear waves that have drawn the most attention for decades. They occur in widely diverse physical and mathematical settings. They are spatially localized, or "solitary,"

waves that behave similarly to particles, as suggested by the suffix "-ton" in "soliton," usually with a bell-shaped profile similar to a Gaussian probability density function. Their first noteworthy feature is that a soliton will propagate indefinitely with no change in profile or speed and a breather will oscillate in place, like a standing wave, indefinitely without change in shape. They do not emit power. Solitons and breathers also emerge naturally from rather arbitrary initial disturbances.

A soliton is a perfect balance between two effects. One tends to steepen any nonlinear, localized pulse and the other to broaden any localized pulse over time. Any acoustic, electromagnetic, or other kind of pulse obeying a nonlinear wave equation has a tendency to change its shape over time. Eventually it should form a shock or discontinuity at its leading or trailing edge because regions of the pulse with different amplitudes travel at different speeds. Depending on the situation, the main peak may overtake the leading edge or the trailing edge may catch up to the peak.

As an ocean swell nears the shore, for example, eventually the amplitude of the wave becomes comparable to the water depth. This causes the crest to outpace the leading edge, so the leading edge steepens until the wave becomes unstable and crashes. Cars on a freeway can show the opposite behavior. If the density of cars is a maximum in the middle of a group of them, then when the group slows down, the speed of those at the trailing edge, where the density is relatively small, will exceed the speed of the denser ones in the middle of the group. A shock can form as cars at the rear of the packet overtake the center of the group.

The other effect is the tendency of any localized wave, linear or nonlinear, to broaden over time. This is because a pulse contains a mix of frequencies and different frequencies have different phase-velocities, with the sole exception of light traveling in vacuum. This pulse-broadening is called "dispersion."

Dispersion is not to be confused with diffraction, which is also called "interference" or "beating." This occurs when waves get in step or out of step and it leads to either constructive addition when they are "in phase" or destructive cancellation when they are "out of phase." Dispersion produces the striking prismatic effects in rainbows and diamond rings where different colors, by Snell's law, are refracted at different angles. Interference can produce similar effects, such as the rainbow in sunlight reflected from a thin film of oil and the wall of a soap bubble. Diffraction holds a special place in history. It was demonstrated by Thomas Young (1801) in an experiment that finally laid to rest the long-standing question of whether light was made of waves or particles. Newton (1642 - 1727) had guessed particles.

Solitons and breathers are called "particlelike" because of their second noteworthy and even more remarkable feature: they emerge from collisions delayed but unchanged in shape and speed. This is amazing, for they do not obey the principle of linear superposition. They have no apparent excuse to pass cleanly through each other after having interacted nonlinearly. Yet they do indeed have a firm opinion about their shape. The reason for particlelike behavior is far from obvious.

The first reported observation of a soliton was in 1834. John Scott Russell, a Scottish civil engineer and naval architect, noticed a solitary hump emerge from the roiling water at the bow of horse-drawn canal-barge as it came to a halt [4, 5]. Russell, on horseback, followed it for miles until losing it "in the windings of the canal." The true nature of solitons remained a mystery for over a century. The equation for surface waves on water of finite depth that governs the wave Russell observed is called the Korteweg-deVries (KdV) equation. It was derived first by Boussinesq [6] in 1877 and again independently by Korteweg and deVries [7] in 1895.

A breakthrough in soliton theory occurred in 1967. Interest in them has expanded dramatically ever since. That year saw the discovery of the inverse scattering transform (IST) and its application to solve the KdV equation [8]. ISTs allow the solution of the three most basic nonlinear wave equations [9], in addition to others, by a series of linear, though nontrivial, steps. An IST explains particlelike behavior. It also shows

that breathers are bound soliton–anti-soliton states corresponding to complex-conjugate eigenvalues in the corresponding IST. Within six years, ISTs were found for the other two most basic nonlinear wave equations, namely the nonlinear Schrödinger (NLS) [10] and sine-Gordon (SG) [11] equations in 1972 and 1973, respectively. We do not address the situations where these equations arise, but the SG equation is a particular Klein-Gordon equation whose breather is the closest true breather to the pseudobreathers treated here. The name "sine-Gordon," by the way, is a play on words.

ISTs are not directly relevant to the work reported here and cannot be adequately described in few words, but it is worthwhile to offer remarks about them for general interest. One may be familiar with the time-independent Schrödinger equation. This governs the quantum mechanical behavior of a particle with a fixed energy in a potential well. It also gives the probability that a particle with a certain energy or momentum incident on a potential well or barrier will be reflected from it or transmitted through it.

We learn in quantum mechanics that a particle in a potential well can have only certain discrete energies or "eigenvalues" in discrete "states," resembling the discrete modes of a vibrating string clamped at each end. We also learn that there is a certain probability that a particle with a given energy or momentum incident on a potential barrier or well will be reflected from it or transmitted through it. The student might be asked to estimate the probability that a piece of tissue paper will reflect a tank and that a tank with too little energy to coast over a hill might get to other side by quantum mechanical "tunneling." The probability of either event is of course fantastically small.

Suppose that $u(x,t)$ satisfies a nonlinear wave equation such as those just mentioned, or specifically the KdV equation, with $x$ and $t$ denoting distance and time, respectively. For these special nonlinear wave equations, if $u(x,t)$ is taken to be the potential, meaning the height of either a well or a barrier, in the time-independent Schrödinger equation, with $t$ regarded simply as a parameter rather than time in the quantum problem, then it turns out, miraculously, that the eigenvalues are independent of time. It also turns out that, if one knows how the coefficients of reflection and transmission depend on the incident momentum or energy of the particle, then one can deduce the scattering potential itself, in other words, $u(x,t)$. This is called the "inverse scattering problem." It is reasonable that the scattering data suffice to reconstruct the scattering potential.

In Ahort, an IST combines the above Adeas to Aeduce $u(x,t)$, Aiven Ats assumed Anitial asymptotic behavior, Auch as Ats vanishing along with Ats Aerivatives as $x \to \pm\infty$. In Aeneral, there As Ao way to determine *a priori* whether a Aiven Aonlinear wave Aquation Aven Aas a corresponding Acattering problem. Aach Aonlinear wave Aquation As treated Aifferently. The Schrödinger Aquation As Aot the only scattering Aodel used to construct ISTs. We cited At because At As Aost Aikely to be AamiliAr and was used to Aolve the KdV Aquation when the IST was Antroduced. According to Aegend, the Aevelopment of the IST resulted Arom a Aallway conversation on Aonlinear waves that was overheard by Aomeone familiar with the Anverse Acattering Aroblem.

In the following, we use the adjective "true" for solitons and breathers that are exact solutions of nonlinear wave equations obtained by an IST. As noted, true solitons and true breathers emerge from collisions with no change in their shape or speed and do not radiate.

The KG equations studied here do not possess ISTs, so they do not have true soliton or breather solutions [12]. The pseudobreathers treated here are only breatherlike solutions of nonlinear KG equations. We assume they oscillate sinusoidally in order to initialize them, but they do not vibrate sinusoidally. In order to initialize them, we just ignore harmonics (multiples of the fundamental frequency). Our pseudobreathers are not stable, but are found to decay very slowly at small to moderate amplitudes.

The author's 1977 PhD dissertation [13] simulated the reflection of intense narrowband electromagnetic planewave pulses normally incident on an inhomogeneous, cold, collisionless electron plasma with a

linearly increasing density. The simulations took into account the increase of an electron's mass with speed, a relativistic, nonlinear effect. This problem was modeled with a saturable KG equation. The reflected pulse left behind long-lived, localized, breatherlike blobs in the so-called "overdense" region of the plasma, deeper than a linear wave could penetrate. This work was unrealistic in ignoring the Lorentz force on the electrons, but the trapped blobs resembled the well known phenomenon of plasma "cavitons." This was followed in 1987 by an article on simulations of another saturable KG equation [14], this one governing a positively charged string vibrating perpendicularly to a pair of parallel, fixed, negatively charged lines in the midplane of the latter.

In 1985, while working with the author as a New Professional, R. Forni found an exact breatherlike solution for a string in a V-shaped trough. This is an idealized system. It is not physically unrealizable. Forni's solution is the simplest breather, though not a true breather. His solution will not be displayed here, but it consists of simple quadratic algebraic forms. Forni's solution was not published until 2018 [15].

Forni's breather oscillates nearly sinusoidally. It contains odd harmonics (multiples) of the fundamental frequency. The amplitude, or Fourier coefficient, for the waves at each of these frequencies turns out to be proportional to the reciprocal of the cube of its harmonic number. Parseval's theorem says the power or energy at each frequency is proportional to the square of its Fourier coefficient, which means that the power or energy in the odd harmonics is proportional to the inverse of the sixth powers of the odd integers. The end result is that about $0.14\%$ of the total energy lies in the harmonics. This follows from an identity equivalent to Parseval's theorem that reads [16]

$$1+\frac{1}{3^6}+\frac{1}{5^6}+\frac{1}{7^6}+\cdots=\frac{\pi^6}{960}\simeq 1.00144707$$

We do not simulate Forni's solution here. In fact, it cannot be simulated, but its nearly sinusoidal nature accounts for the success of the approximation of sinusoidal motion that we use to initialize the pseudobreathers (see Section 3), meaning their long lifetime and particlelike behavior. A few remarks on Forni's solution follow.

When it is stationary, at its maximum displacment, Forni's blob has a bell-curve shape made up of linked parabolas. There is a center region with negative curvature and two symmetric tails with equal but positive curvature. These meet at the half-maximum. The tails fall to zero when their slope (or "derivative with respect to $x$") is equal to zero. Beyond these points, the blob vanishes. Breathers that vanish identically outside of some region, incidentally, are called "compactons."

The slope of Forni's solution is everywhere well defined, but initially its curvature (or "second derivative with respect to $x$") is discontinuous at the point half-way down from the peak where the parabolas meet. This corresponds to the point of inflection for a Gaussian or "normal" bell-curve, at which the curvature is equal to zero.

As the string falls from maximum displacement, part of it takes on an expanding, linear (straight line) shape spreading out from the half-maxima. As it falls, the parabolic regions shrink and are replaced by expanding linear regions that rotate as they fall. When the string crosses the bottom of the trough, the linear region extends from the center of the blob where $x=0$, say, out to each edge and at this instant the speed of the string is a maximum at $x=0$ and decreases linearly until it vanishes at the edges.

There is an electrostatic analog for Forni's nonphysical mechanical system. The electric field produced by a uniformly charged plate of infinite extent is perpendicular to the plate and independent of distance from the plate. Forni's model has a string in a V-shaped trough under the force of gravity, but this string obeys exactly the same form of wave equation as a string with a uniform positive charge density that

oscillates perpendicularly to a pair of semi-infinite, coplanar, uniformly negatively charged fixed plates through an infinitesimal gap or slit that separates them.

In other words, the restoring force is constant on either side of the trough or either side of the plates for sufficiently thin plates. It vanishes when the string is at the bottom of the trough or in the plane of the plates and it changes sign discontinuously when the string crosses the bottom of the trough or the plane of the plates. The restoring force, as a function of the string's displacement from equilibrium, is an inverted, shifted step-function, like a single step going down a flight of stairs.

Around May, 2017, the author noticed that this electrostatic analog suggests a generalization of Forni's nonphysical mechanical system that gives a realizable system. One can widen the infinitesimal gap between the plates and have a gap of finite width as shown in Fig. 1. It turns out to be possible to compute the electric field of the plates along the $z$-axis. It is proportional to $\tan^{-1}(z/a)$, which is a smoothed, odd, step-function that goes from $-\pi/2$ to $\pi/2$. We do not pause to derive this formula, nor have we found it in texts, but the derivation is like standard potential-theory problems in introductory electricity and magnetism courses.

Simulations of the nonlinear KG equation for the system in Fig. 1 were first carried out in December, 2017, showing particlelike pseudobreathers existed. This motivated the long-delayed publication of Forni's solution, including examples of colliding pseudobreathers for the system in Fig. 1.

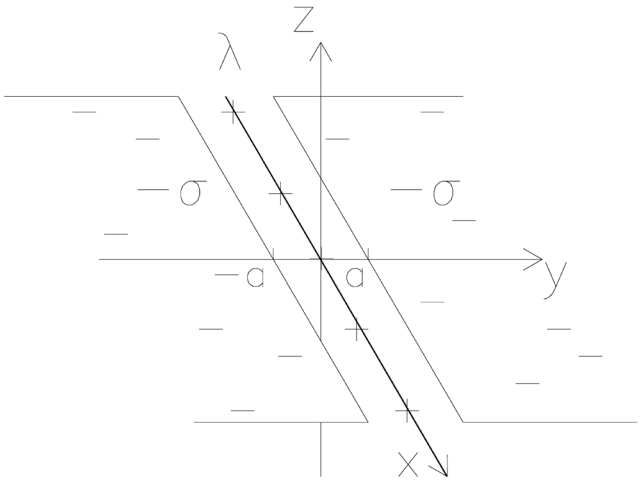


Figure 1. This cut-away view shows a string with uniform linear charge density $\lambda > 0$ that lies on the $x$-axis in equilibrium and is assumed to vibrate in the $xz$-plane. The string can be a strip for rigidity against motion out of the $xz$-plane. Two semi-infinite plates in the $xy$-plane with surface charge density $-\sigma < 0$ separated by a gap of width $2a$ produce an electric field equal to $-4\sigma \tan^{-1}(z/a)$ along the $z$-axis.

KG equations are uniquely important because they describe phenomena consistently with special relativity, as discussed below, unlike the great majority of other nonlinear wave equations that have attracted intense interest. Pseudobreathers in saturable KG equations are particularly appealing because their self-trapping has a simple, intuitive explanation. It involves the idea of a cut-off frequency, meaning a frequency below which waves cannot propagate. For example, there is a cut-off frequency of about $10$

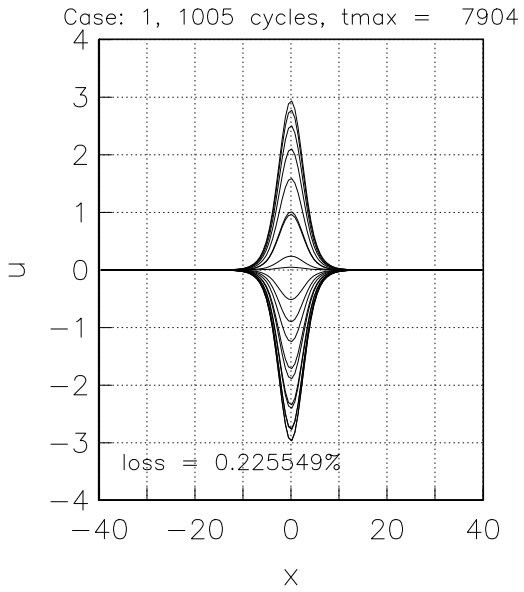


Figure 2. For the system in Fig. 1 and second potential in Eqs. (12) in Section 2.3, twenty-one snapshots equally spaced in time for a pseudobreather with amplitude 3 are shown over 1005 cycles. The energy loss is about $0.2255\%$.

MHz for electromagnetic waves in the earth's ionosphere. The result is that microwave signals with carrier frequencies smaller than about $10$ MHz are reflected, thus letting ham radio operators talk over the horizon.

We find that pseudobreathers with small to moderate amplitudes decay extremely slowly. Figure 2 shows this for the second potential in Eqs. (12) in Section 2.3, which governs the system in Fig. 1. It shows twenty-one snapshots equally spaced in time over 1005 cycles, as seen from above, looking down into the equivalent trough. The blob has lost about $0.2255\%$ of its initial energy over this time.

We also find that, unlike true solitons or true breathers, pseudobreathers exchange small amounts of energy and momentum in collisions, while retaining their shape to high accuracy, as shown in Fig. 3. Their weak interaction is extremely interesting, for it might lead to novel nano-scale electrostatic, magnetostatic, mechanical, or other devices for memory or computation (classical or quantum), possibly including nanotubes, providing an alternative to the size-limitations of present semiconductor devices.

We close this section with a remark on initializing collisions, anticipating Section 3 to mention one of the aesthetic aspects of pseudobreathers. Collisions between solitons are simple to set up because solitons are known functions. Breathers, however, are like standing waves and need not move. How does one make a breather move? The answer is that the relativistic nature of KG equations, formally their "Lorentz invariance," makes it straightforward to initialize a moving pseudobreather, assuming that in its own rest frame it has the form $u(x)\cos\omega t$. The scheme uses a Lorentz transform, as discussed in Section 4.

The idea is that the mathematical form of a KG equation is unchanged when the original variables for space and time, say $x$ and $t$, respectively, in one reference frame are expressed in terms of the space and time variables, say $x'$ and $t'$, respectively, in another frame in motion relative to the first frame. The original unprimed variables denote the location of a point in space and time, or an "event," as seen by people on the ground, say, and the primed variables denote the location of the same event as seen by people on a train. Special relativity shows how these variables are transform between frames. The frame-to-frame transformation is called a Lorentz transform. A Lorentz transform mixes or intertwines space and time. Section 4 gives the equations and discusses their physical meaning.

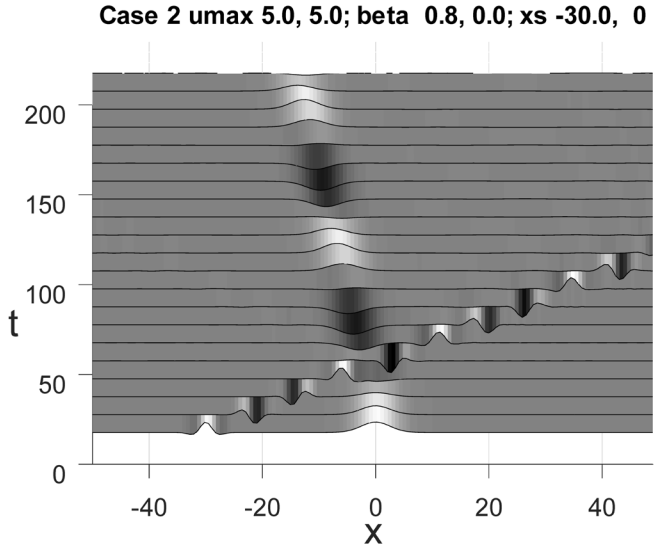


Figure 3. A collision is shown between an incident blob initially at $x = -30$ with speed $0.8$ and a stationary target blob initially at $x = 0$, both of amplitude 3, for the system in Fig. 1.

Mathematically, this idea reads $(\partial/\partial t)^2 - c^2(\partial/\partial x)^2 = (\partial/\partial t')^2 - c^2(\partial/\partial x')^2$, an identity between partial derivatives. The invariance of the operator just displayed has a simple interpretation. It means that the string obeys the same wave equation in each frame. The Lorentz transform of variables from the train-frame to ground-frame lets us deduce what we, as observers on the ground, see when we watch a breather that is stationary in the eyes of observers on a moving train.

The speed of waves on a free string, denoted $c$ in the equation above, corresponds to the speed of light in vacuum. The Principle of Relativity, the sole assumption in the theory of special relativity, states that the laws of nature are the same in every reference frame, and our string obeys this rule. Of course, $c$ is many orders of magnitude smaller than the speed of light in vacuum. We are not treating a relativistic string.

Section 2 sets out the basic mathematics, with Section 2.1 on KG equations. These are almost the simplest form of wave equation. As mentioned, they govern other systems besides a classical mechanical string subject to an external conservative restoring force, such as electromagnetic waves in a conducting medium, as shown in Section 2.2. Section 2.3 lists the six potential energy functions or trough cross sections studied here. Section 2.4 gives an intuitive explanation for a pseudobreather's self-trapping.

Sections 3, 4, and 5 discuss, respectively, the numerical methods used for initializing pseudobreathers at rest, boosting (Lorentz transforming) them, and simulating them. Section 6 addresses decay and collisions and Section 7 provides final comments.

Solitons and breathers are not candidates for elementary particles such as electrons, neutrinos, photons, and quarks. The term "breather" is perhaps misleading, for breathers do not expand and contract like an accordion. It is unclear who coined the term "breather" and when. It seems to date from the discovery of the ISTs for the NLS and SG equations (1972 and 1973, respectively).

# 2. MATHEMATICAL BASICS

## 2.1 WAVES ON A STRING AND THE CUT-OFF FREQUENCY

To a first approximation, a string free of external forces, having a uniform linear mass density $\rho$ and tension $T$, and with transverse displacement $u(x,t)$ in a plane from its equilibrium position, obeys

$$\rho u_{tt} - T u_{xx} = 0\,, \tag{1}$$

where $x$ denotes distance along the string, $t$ denotes time, and subscripts denote partial derivatives. This is the basic wave equation introduced in engineering and physics courses. It ignores heat owing to internal friction or stiffness of the string.

Equation (1) is Newton's Second Law, namely $F = ma$ (force is equal to mass times acceleration) in the nonrelativistic case, expressed per unit length for a string. That is, the first term is the product of the mass per unit length and the transverse acceleration. The second term is (minus) the transverse force per unit length. This force is proportional to the tension $T$ and to the curvature (or second derivative with respect to $x$) of the string.

We do not pause to derive the expression $Tu_{xx}$ for the force per unit length in Eq. (1), but will merely point out why it makes sense. If a tiny element of length along the string were straight, then the total force on it would have to vanish. This is because the force of tension on each end of it would balance or cancel out. But if the element were slightly bent, then the forces of tension on its ends would not be antiparallel and would not balance. Regardless of the sign of the slope, positive curvature is an upward bend resembling a smile and produces a net upward transverse force, while negative curvature resembling a frown produces a net downward transverse force.

The equation $F = ma$ is called Newton's Second Law, but it is not a law of nature, nor is its relativistic generalization, $F = d(mv)/dt$, in which the mass $m$ is allowed to depend on speed. This misunderstanding seems to be widespread. Newton's Second Law is the definition of force as the rate of change of the momentum of a body (its mass times its velocity), assuming mass and velocity are already defined. It cannot be put to a test experimentally, for it holds by definition. In contrast, a law of nature, whether established or just proposed, can be tested by experiment. We can test the formulas for the gravitational force between two masses, the electrostatic force between two charges, the magnetic field produced by a current in a wire, and the radiation from an oscillating point-charge.

Equations of the form of Eq. (1) also govern compressional, or so-called "longitudinal" acoustic waves and transverse electromagnetic waves. Although it is called a "wave equation," solutions of Eq. (1) need not oscillate. Any function $u(x,t)$ whatsoever that depends on $x$ and $t$ in the combination $x - ct$ or $x + ct$ is a solution, where $c = \sqrt{T/\rho}$. This represents a fixed profile moving at speed $c$ to the right or left, respectively. There is no dispersion, and $c$ may be the speed of light in vacuum, the speed of sound in air or any other medium, or the speed of waves on a free string.

If the string is subject to a conservative external force $f(u)$ per unit length, then it obeys the equation

$$\rho u_{tt} - T u_{xx} = f(u)\,. \tag{2}$$

For future convenience, note that this can be rewritten as

$$u_{tt} - c^2 u_{xx} = f(u)/\rho\,, \tag{3}$$

in which each term has the dimensions of acceleration.

The energy, momentum, and power flow along the string will be addressed in Section 5. We note, however, that Eq. (2) conserves energy and that the energy takes three forms. A free string has kinetic and potential energy. The latter arises from the work needed to stretch the string in any region where it has a nonzero slope. To a first approximation (for small slopes), this energy, per unit distance, is proportional to the square of the string's slope at any point along it. We omit the proof. Equations (2) and (3) have the form called "Klein-Gordon" for one dimension.

The external force $f(u)$ has an associated conservative potential energy per unit length, which we denote by $V(u)$. These two functions are related by the equation $f(u) = -dV(u)/du$, a basic relationship that will be used repeatedly below, so we pause to comment on its meaning. Let $u$ denote the position of a body, such as a tiny element of length along a string. If the force $f(u)$ pushes or pulls on this body over a tiny distance $du$, then by definition the amount of work it does on the body, say $dW$, is $dW = f(u)du$.

If $dW > 0$, the force does positive work on the body and the body gains this amount of kinetic energy and loses this amount of potential energy, conserving its total energy. The quantity $dW$ may have either sign or vanish and in general must be equal to the negative of the change in the potential energy of the body, giving $f(u)du = -dV(u)$, or $f(u) = -dV(u)/du$, as claimed. For example, the force $F$ of gravity in the vertical direction on an object with mass $m$ is given by the equation $F = -mg$, where $g$ denotes the acceleration of gravity. The corresponding gravitational potential energy $V(y)$ is given by the equation $V(y) = mgy$, with $y$ denoting its height with respect to some arbitrarily chosen origin. These functions obey $F(y) = -V'(y)$.

In the simplest case, $f(u)$ is directly proportional to $u$. Then Eq. (2) is linear. That is, if $u_1(x,t)$ and $u_2(x,t)$ are two solutions of Eq. (2), then $Au_1(x,t) + Bu_2(x,t)$ is also a solution, where $A$ and $B$ are any two constants. This reiterates our description of linear waves in Section 1. This case is the basic point of reference or touchstone for understanding the self-trapping nature of pseudobreathers. As noted, the idea of a "cut-off frequency" is central.

Suppose that $f(u)/\rho = -\omega_0^2 u$ for some real constant $\omega_0$, an angular frequency (radians per second). This is Hooke's law, that is, a linear restoring force, and arises when the string is in a parabolic trough under the force of gravity or embedded in solid rubber or some similar elastic medium. For this case, Eq. (3) reads

$$u_{tt} - c^2 u_{xx} = -\omega_0^2 u\,. \tag{4}$$

Solutions of this equation can be sinusoidal oscillations or decaying or growing exponentials. Its general solution, a sum of forward- and backward-going traveling waves, may be written as

$$u(x,t) = Ae^{i(kx-\omega t)} + Be^{-i(kx-\omega t)} + Ce^{i(kx+\omega t)} + De^{-i(kx+\omega t)}\,, \tag{5}$$

where $i = \sqrt{-1}$, and $A$, $B$, $C$, and $D$ are arbitrary constants. When $k$ and $\omega$ are real, the symbol $k$, called the "wavenumber," is equal to $2\pi$ divided by the wavelength and the symbol $\omega$, called the "angular frequency," is equal to $2\pi$ divided by the period. In the following, we will call $\omega$ the "frequency," with the understanding that "angular frequency" is meant.

The phases in the exponents in Eq. (5), $\pm(kx \pm \omega t)$, can be written as $\pm k[x \pm (\omega/k)t]$, showing that a phase can be constant if $x = \mp(\omega/k)t + a$, for some real constant $a$. If $\omega$ and $k$ are real, then the speed of the phasefronts is therefore $\pm\omega/k$. The quantity $\omega/k$ is called the "phase velocity," and denoted $v_p$. Here the word "velocity" is understood to mean a scalar, not a vector. To be consistent, it should be called the "phase speed," but "phase velocity" has become standard.

With suitable choices for $A$, $B$, $C$, and $D$, the right-hand side of Eq. (5) represents real sinusoidal waves or exponential functions. We could equally as well have written the general solution of Eq. (4) in terms of sines and cosines with arbitrary complex coefficients, but complex exponentials often simplify calculations.

Physical quantities are, of course, always real. But one might ask, as an aside, whether $i$ is known to nature. Does $i$ arise naturally similarly to $\pi$? The author thinks that $i$ is a creation of the mind.

On substituting any of the four terms or their sum on the right-hand side of Eq. (5) into Eq. (4), one finds the relationship between $k$ and $\omega$,

$$c^2k^2 = \omega^2 - \omega_0^2. \tag{6}$$

This is just Eq. (4) with the second derivative with respect to $t$ replaced by $-\omega^2$ and the second derivative with respect ot $x$ replaced by $-k^2$, after cancelling the common factor $u(x,t)$ throughout and rearranging terms. Equation (6) is called a "dispersion relationship" because it is equivalent to a formula for the phase velocity $v_p = \omega/k$ as a function of either $k$ or $\omega$. By definition, $v_p = c/n$, where $n$ is the index of refraction (about 1.3 for visible light in ordinary water). Equation (6) gives

$$\frac{\omega}{k} = v_p = \frac{c}{n} = \frac{c}{\sqrt{1-(\omega_0/\omega)^2}}\,. \tag{7}$$

Equation (6) says that if $\omega > \omega_0$, then $k$ is real. By Eq. (5), $u(x,t)$ is then a sinusoidal function of $x$ and $t$. As $\omega$ approaches $\omega_0$, $k$ approaches 0, meaning that the wavelength approaches $\infty$. If $\omega = \omega_0$, then $k = 0$, and hence $u(x,t)$ is independent of $x$, implying that the string is straight. In this case, the string oscillates from side to side in the trough, remaining parallel to its resting position on the $x$-axis. It acts like a rigid rod or a single point-mass. It oscillates at $\omega_0$, the resonant frequency of the trough. Finally, if $\omega < \omega_0$, then $k$ is imaginary, and according to Eq. (5), $u(x,t)$ is an exponential function of $x$. It can be an increasing or decreasing function of $x$, since we are free to choose the sign of $ik$. It can be shown that in this case the average power flowing along the string vanishes.

For this reason the resonant frequency $\omega_0$ is also called the "cut-off frequency." That is, to have power flowing along the string, $\omega$ must exceed $\omega_0$. The frequency of a pseudobreather is smaller than the cut-off frequency for small-amplitude, linear waves. The small-amplitude wings or tails therefore act as mirrors, explaining why a pseudobreather is self-trapped. This effect is well known.

We let $x$ and $t$ be dimensionless from here on. The symbols $x$ and $t$ can always be scaled (multiplied by constants) to obtain new dimensionless variables. In Eq. (4), for example, we would let $x' = \omega_0 x/c$ and $t' = \omega_0 t$ represent a dimensionless distance and time, respectively. With these variables, the KG equation reads

$$u_{t't'} - u_{x'x'} = f(u)\,. \tag{8}$$

### 2.2 Electromagnetic Waves

Here it is shown that Eqs. (4) and (8) also govern electromagnetic waves in a conducting medium such as a cold, collisionless, electron plasma (ionized gas), taking the earth's ionosphere as an example. We first derive the wave equation for the vector potential. In the centimeter-gram-seconds – electrostatic units (cgs-esu) system, Maxwell's equations in vacuum read

$$\bigtriangledown \cdot \mathbf{E} = \rho\,, \tag{9a}$$

$$\bigtriangledown \cdot \mathbf{B} = 0\,, \tag{9b}$$

$$\bigtriangledown \times \mathbf{E} = -\frac{1}{c}\frac{\partial \mathbf{B}}{\partial t}\,, \tag{9c}$$

$$\bigtriangledown \times \mathbf{B} = \frac{1}{c}\frac{\partial \mathbf{E}}{\partial t} + \frac{4\pi}{c}\mathbf{J}\,, \tag{9d}$$

returning to the customary notation for partial derivatives. Here $c$ is the speed of light in vacuum, $\mathbf{E}$ and $\mathbf{B}$ are the electric and magnetic fields in statvolts/cm, respectively, $\rho$ is the charge density in statcoulombs per cubic centimeter, and $\mathbf{J}$ is the current density in statamps per square centimeter.

The cgs-esu system is preferable to the MKS (meter-kilogram-second) system for theoretical work. In cgs-esu, $c$ is the only constant in Maxwell's equations. The constants $\epsilon_0$ and $\mu_0$ that appear in the corresponding MKS formulas do not appear. In cgs-esu, the radial component of the electric field at distance $r$ from a point-charge $q$ is simply $E = q/r^2$. In cgs-esu, $\mathbf{E}$ and $\mathbf{B}$ have the same units and the unit of energy is the erg (one dyne-cm). The electronic charge is about $1.6 \times 10^{-19}$ Coulombs in MKS and about $4.8 \times 10^{-10}$ esu in cgs-esu. It turns out that one statvolt is equal to 300 volts.

With $\mathbf{A}$ denoting the vector potential, meaning that we let the magnetic field be $\mathbf{B} = \bigtriangledown \times \mathbf{A}$, we automatically satisfy Eq. (9b). With $\rho = 0$, we can let the electric field be $\mathbf{E} = -(1/c)\partial\mathbf{A}/\partial t$, which automatically satisfies Eq. (9c).

For a linearly polarized planewave, we may assume $\mathbf{A} = A\hat{\mathbf{x}}$, where $\hat{\mathbf{x}}$ is the unit vector in the $x$-direction. Then $\mathbf{E}$ is also in the $x$-direction. We need not make an explicit choice for the axes along which the wave propagates and the direction in which $\mathbf{B}$ points. Assuming that $\mathbf{J}$ is parallel to $\mathbf{E}$, on substituting the above expressions for $\mathbf{E}$ and $\mathbf{B}$ into Eq. (9d) we get

$$\frac{1}{c^2}\frac{\partial^2 A}{\partial t^2} - \frac{\partial^2 A}{\partial x^2} = \frac{4\pi}{c} J\,, \tag{10}$$

where $A$ and $J$ denote the $x$-components of the vector potential and current density, respectively. This has the form of a KG equation. The interpretation of this equation is that $J$ is the source of radiation. Given $J$ and the initial and boundary conditions, Eq. (10) determines $\mathbf{A}$. For example, given the oscillating current in a line-antenna, one can determine how it radiates using Eq. (10). If the current flowed steadily in a circular loop, we could determine the static magnetic field resembling a dipole field at large distances. We have said nothing yet about how or whether $\mathbf{J}$ depends on the fields themselves. This so-called "constituitive relation" is different in each medium. We now consider a particular situation.

In the simplest model for a plasma, positive ions are treated as fixed owing to their much greater mass than free electrons and both collisions between particles and the Lorentz force $q(\mathbf{v}/c) \times \mathbf{B}$ on electrons are ignored. Free electrons then obey the equation of motion $ma = q\mathbf{E}$, where $m$ is the mass of an electron, $q$ its charge, and $a$ its acceleration. Since $a = dv/dt$, with $v$ denoting speed, this reads $m\,dv/dt = -(q/c)\partial A/\partial t$, and hence $mv = -qA/c$, or $v = -qA/mc$.

The current density is given by $J = nqv$, where $n$ denotes the number density of free electrons (the number of free electrons per cubic centimeter). The plasma is assumed to be electrically neutral, so that $\rho = 0$, but free electrons move. Substituting the expression for $v$ into the expression for $J$ gives $J = -nq^2A/mc$. Substituting this in turn into Eq. (10) and multiplying throughout by $c^2$ yields

$$\frac{\partial^2 A}{\partial t^2} - c^2\frac{\partial^2 A}{\partial x^2} = -\frac{4\pi nq^2}{m} A\,, \tag{11}$$

which is of the form of Eq. (4), with $\omega_0^2 = 4\pi nq^2/m$ being the (squared) cut-off freqency. The quantity $\omega_0$ is called the "plasma" or "Langmuir" frequency.

In the expression for $\omega_0$, increasing $m$ is equivalent to decreasing $n$. The relativistic increase of an electron's mass with its speed in the author's dissertation [13] is thus equivalent to a caviton, that is, a region of low ion density that acts as a cavity resonator. Another similarity is that, since an electron's speed is limited by the speed of light, the current density $J$ saturates in the limit of infinite intensity, which mimics the lower bound of zero ion density.

The maximum number density $n$ of free electrons is $10^5 - 10^6/\,\mathrm{cm}^3$ in the ionosphere. The electronic charge in cgs-esu, as noted above, is $q \simeq 4.8 \times 10^{-10}$ esu, and the electronic mass is $m \simeq 9.1 \times 10^{-28}$ g. These values give cut-off freqencies (in Hertz) of $3 - 9$ MHz.

The Lorentz force $q(\mathbf{v}/c) \times \mathbf{B}$ on electrons was neglected above because $\mathbf{v}$ is proportional to $\mathbf{A}$, implying that the Lorentz force scales as the square of the field-strength or, equivalently, as the square of the speed $v$. To include the Lorentz force self-consistently, one should therefore also include a relativistic correction for the electron's mass. Since the Lorentz force is perpendicular to $\mathbf{E}$ and $\mathbf{B}$, it would also be necessary to allow electrons to move in the direction of propagation of the planewave, that is, in the direction of Poynting's vector $\mathbf{S} = (c/4\pi)\mathbf{E} \times \mathbf{B}$.

### 2.3 Potentials, Forces, and Frequencies

The potential energy functions we have investigated, shown in Fig. 4, are as follows, in order of decreasing steepness, or equivalently, increasing width.

$$V_1(u) = \left[1 - \left(\frac{2}{\pi}\tan^{-1}\frac{u}{5}\right)^2\right]\frac{1}{2}u^2\,. \tag{12a}$$

$$V_2(u) = u\tan^{-1}u - \frac{1}{2}\ln(1+u^2)\,, \tag{12b}$$

$$V_3(u) = \ln(\cosh u)\,, \tag{12c}$$

$$V_4(u) = \frac{1}{2}\left[1+\cos\left(\frac{\pi u^2}{1+u^2}\right)\right]\frac{u^2}{2} + \frac{1}{2}\left[1-\cos\left(\frac{\pi u^2}{1+u^2}\right)\right](\sqrt{1+u^2}-1)\,, \tag{12d}$$

$$V_5(u) = \sqrt{1+u^2} - 1\,, \tag{12e}$$

$$V_6(u) = [1-\mathrm{erf}^2(1.5u)]u^2/2 + \mathrm{erf}^2(1.5u)(\sqrt{1+u^2}-1)\,. \tag{12f}$$

The function erf, a smoothed step-function from $-1$ to 1, is defined by

$$\mathrm{erf}(x) = \frac{2}{\sqrt{\pi}}\int_0^x e^{-t^2}dt\,.$$

The corresponding forces, given by $f_i(u) = -V_i'(u)$ and shown in Fig. 5 below, are as follows:

$$f_1(u) = \frac{4}{5\pi^2}\frac{u^2}{1+(u/5)^2}\tan^{-1}\frac{u}{5} - \left[1-\left(\frac{2}{\pi}\tan^{-1}\frac{u}{5}\right)^2\right]u\,, \tag{13a}$$

$$f_2(u) = -\tan^{-1}u\,, \tag{13b}$$

$$f_3(u) = -\tanh u\,, \tag{13c}$$

$$\begin{aligned} f_4(u) = {} & \frac{\pi u}{(1+u^2)^2}\sin\left(\frac{\pi u^2}{1+u^2}\right)(\frac{1}{2}u^2 - \sqrt{1+u^2}+1) \\ & -\frac{1}{2}\left(u + \frac{u}{\sqrt{1+u^2}}\right) \\ & -\frac{1}{2}\cos\left(\frac{\pi u^2}{1+u^2}\right)\left(u - \frac{u}{\sqrt{1+u^2}}\right)\,, \end{aligned} \tag{13d}$$

$$f_5(u) = -\frac{u}{\sqrt{1+u^2}}\,, \tag{13e}$$

$$\begin{aligned} f_6(u) = {} & -u + \frac{6}{\sqrt{\pi}}\mathrm{erf}(1.5u)e^{-(1.5u)^2}(\frac{1}{2}u^2 - \sqrt{1+u^2}+1) \\ & +\mathrm{erf}^2(1.5u)(u - \frac{u}{\sqrt{1+u^2}})\,. \end{aligned} \tag{13f}$$

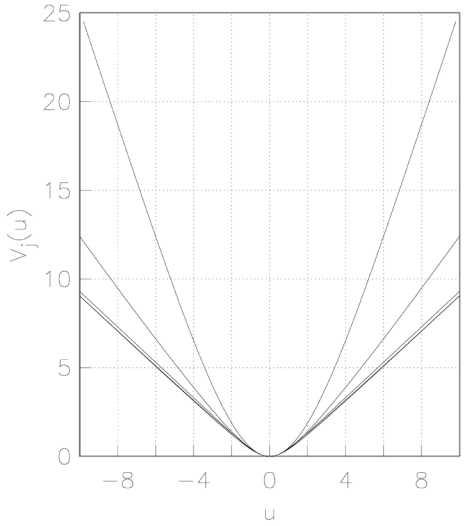


Figure 4. The six potentials per unit distance in Eqs. (12) are shown, with $V_1(u)$ being the uppermost and $V_6(u)$ the lowest.

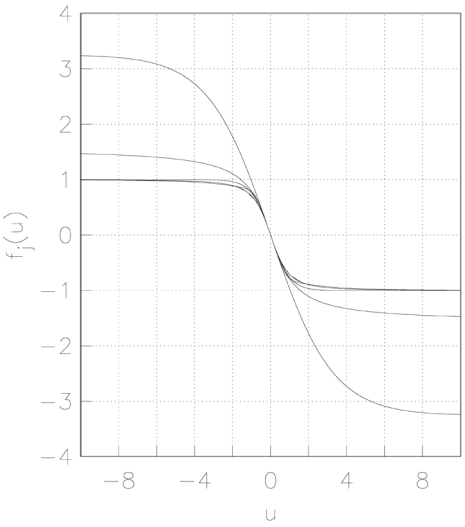


Figure 5. The six forces per unit length in Eqs. (13) are shown, with $f_1(u)$ being the largest and $f_6(u)$ the smallest.

The potentials are normalized such that, as $u \to 0$, each approaches the limiting form $V_j(u) = u^2/2$. As $|u| \to \infty$, each approaches the form $V_j(u) = A|u|$, where $A$ is a positive constant. The second of these describes the physical system in Fig. 1. The others have no immediately obvious corresponding physical system other than a string in a trough under the force of gravity. That is, one may regard the curves in Fig. 4 as cross sections of troughs, with gravity pointing down along the vertical axis. The restoring forces are therefore smoothed, inverted step-functions, that is, they saturate (approach a constant) at large amplitudes. A particle released from a point far up the wall of the trough would have an effectively constant acceleration and be in free-fall.

Figure 6 shows the frequencies $\omega$ and the periods of the pseudobreathers for each case as functions of the amplitude, $u_{\max}$. The frequencies are computed using Eq. (21) below and the period is $2\pi/\omega$.

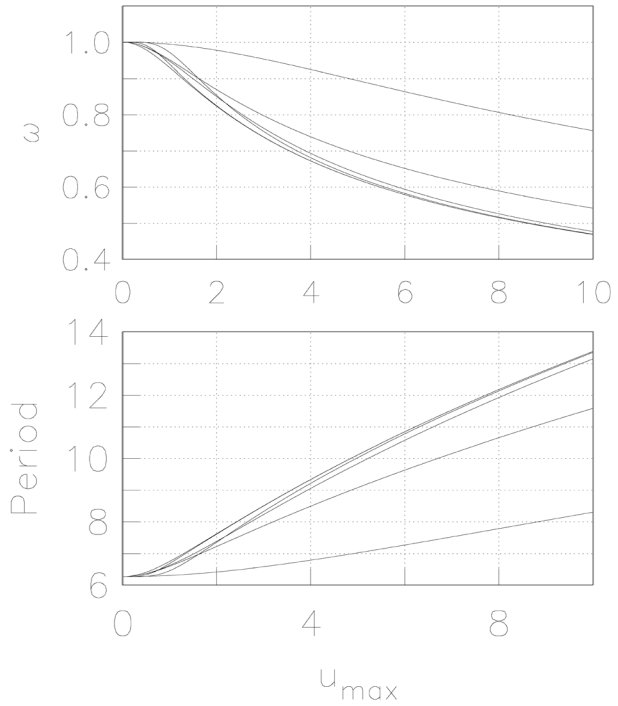


Figure 6. Frequencies $\omega$ and periods of pseudobreathers are shown for each case as a function of the amplitude $u_{\max}$. The first case (the steepest trough) corresponds to the uppermost curve for $\omega$ and lowermost curve for the period. For example, at $u_{\max} = 10$, the largest frequency is $\omega \simeq 0.75$, and $2\pi/0.75 \simeq 6(4/3) = 8$, agreeing with the smallest period.

### 2.4 Self-trapping

A pseudobreather's self-trapping was mentioned following Eq. (7), but is worth revisiting for an intuitive picture. Consider a string in a parabolic trough, so that it obeys the linear Eq. (4) with dispersion relation Eq. (6). Let us pinch the string between two fingers and shake it at some frequency $\omega$. If $\omega > \omega_0$ then $k$ is real and waves will be emitted. Obviously, since the shaking frequency exceeds the resonant frequency, the string cannot keep up with point at which we shake the string. It must lag behind. One can picture the resulting ripples carrying away energy. Our fingers always lead the string. We are always pulling it and continually doing positive work on it.

But if the shaking frequency satisfies $\omega < \omega_0$, then $k$ is imaginary and there is no radiation. Instead, the string oscillates sinusoidally, but the displacement decays exponentially to the left and right of the point of shaking. We pull it up and it pulls us down, with no net work done over a single cycle.

For the potential energy functions we treat, the resonant frequency decreases with increasing amplitude, as noted earlier. A single particle, released from higher and higher, would take longer and longer to complete a cycle. The frequency of a pseudobreather is therefore smaller than the linear resonance or cut-off frequency for small-amplitude waves. This means that the small-amplitude wings or tails of a pseudobreather, which are effectively linear, are driven at a frequency below the cut-off frequency and hence cannot radiate.

This is only approximately true, for the string's vibration is not sinusoidal. A small fraction of its energy is in the odd harmonics that exceed the cut-off frequency, as was noted in the case of Forni's solution. This accounts for the slow decay of pseudobreathers. It is unclear, however, how much power should be radiated

and how quickly a pseudobreather should decay. We address this question by simulating pseudobreathers on a string whose ends are absorbing or reflectionless, as discussed in Section 5.4.

# 3. INITIALIZING A PSEUDOBREATHER

It is impossible to initialize a pseudobreather in a rigorous sense, since, as noted above, true breathers do not exist for our equations [12]. We make the standing-wave approximation $u(x,t) = u(x)\cos(\omega t)$. This assumes pseudobreathers oscillate sinusoidally, but they do not. It is surprising that the initialization method produces blobs as long-lived and particlelike as they are. Note that the symbol $u$ is used with two different meanings here. Which is meant should be clear from the number of arguments.

By ignoring harmonics and assuming sinusoidal motion, we can eliminate time from the wave equation, leaving $x$ as the independent variable. We get an ordinary nonlinear differential equation for $u(x)$, the blob's initial shape. We solve this numerically to find the shape of the blob at its maximum displacement, when it has zero speed.

A mechanical analogy makes the nature of the solution clear. The equation has the same form as Newton's Second Law $F = ma$ for a particle in a double-well potential, with $x$ playing the role of time for the analogous particle. A particle in a double-well potential has three possible types of trajectories. One of these corresponds to the initial profile. We first discuss a particle in a double-well potential, then present the numerical method for solving its equation of motion, and lastly derive the equation for the profile.

### 3.1 Analogous Particle in a Double-Well Potential

Consider a particle of unit mass and position $u(t)$, with $t$ denoting time, in a potential $V(u)$ with two symmetric wells, as shown in Fig. 7 for the case

$$V(u) = \frac{1}{2}\omega^2 u^2 - (\sqrt{1+u^2} - 1)\,,$$

where the constant $\omega$ is inserted here for future convenience and set equal to $0.5$. Note that $V(0) = 0$. The first term on the right-hand side of this equation is a parabola and has curvature $\omega^2$. As $|u| \to 0$, the sum of the second and third terms (including the sign) approaches $-u^2/2$. This has curvature $-1$. Hence, $V(u)$ has a double-well shape provided that $\omega < 1$. If $\omega > 1$, then the curvature of $V(u)$ at $u = 0$ would be positive, whereas it must be negative at $u = 0$ for a double-well.

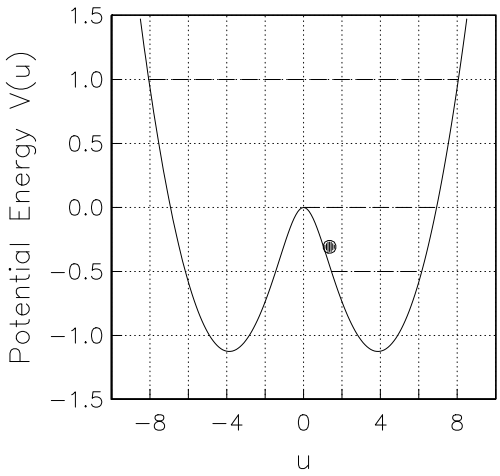


Figure 7. A particle in a double-well potential $V(u)$ is shown. Horizontal dashed lines are at values for the particle's energy that give, from top to bottom, an unbiased periodic oscillation ($E = 1$), a non-oscillatory trajectory ($E = 0$), and a biased periodic oscillation about the minimum of either well at $u \simeq \pm 4$ ($E = -0.5$).

Since the kinetic energy is the difference between the particle's total energy $E$ and $V(u)$, the particle's speed vanishes when $V(u) = E$. This occurs at the turning points of its periodic motion. Depending on the value of $E$, it will follow one of three types of trajectories. If $E > 0$ (top dashed horizontal line in Fig. 7), it makes symmetric or unbiased oscillations about $u = 0$. For $E = 1$, for example, the turning points are at $u \simeq \pm 8$. If $E < 0$, say $-0.5$ (bottom dashed horizontal line), it makes biased oscillations with turning points at $u \simeq 1$ and 6 or their negatives. In each of these cases, the motion is periodic.

One can show that the minima of the double-wells are at $u = \pm\sqrt{15} \simeq \pm 3.87$ and that for $E = 0$, the turning point is at $u = 4\sqrt{3} = 6.928203\ldots$. The case $E = 0$ (middle dashed horizontal line) is different, giving a non-oscillatory trajectory. Instead, $u$ varies between $u = 0$ and $u \simeq 7$ and the trajectory is not periodic. If the particle is at rest at $u \simeq 7$ initially, then it will accelerate downhill towards the origin, reaching maximum kinetic energy when $u \simeq 4$, and approach the origin with diminishing speed. It arrives at $u = 0$ with speed 0 after an infinite time. It will not get over the hill, since its speed vanishes at $u = 0$. The trajectory $u(t)$ vs. $t$ in this case corresponds to the initial shape $u(x, t = 0)$ of our pseudobreather in the region $x \geq 0$, with $x$ playing the role of time in the mechanical analogy. Figure 8 shows the trajectories for the three energies in Fig. 7.

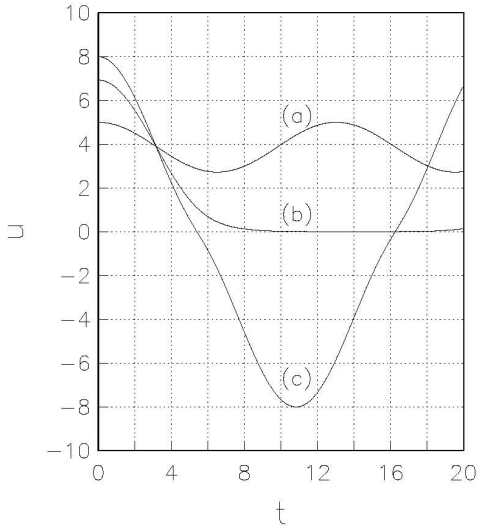


Figure 8. Three trajectories are shown for a particle in the potential in Fig. 7 with initial positions of (a) 5, (b) $4\sqrt{3} \simeq 6.92820323$, and (c) 8. For negative $t$, each curve is the mirror image of that shown.

The particle could also be at rest at $u = 0$ at $t = -\infty$. This is an unstable equilibrium. Borrowing from quantum mechanics, Heisenberg's uncertainty principle guarantees that it won't stay at $u = 0$ forever, and eventually will begin to move. If it happens to move to the right, then it will execute a single to-and-fro motion. There is no loss of generality in letting the particle reach its turning point at $t = 0$. The trajectory $u(t)$ vs. $t$, curve (b) in Fig. 8, then corresponds to the initial shape $u(x, t = 0)$ of a breather, but now on the region $-\infty < x < \infty$, with $x$ playing the role of time in the mechanical analogy as before.

### 3.2 Fourth-Order Runge-Kutta Method

For the choice of $V(u)$ above and for $m = 1$ in $F = ma$, the particle obeys

$$\frac{d^2u(t)}{dt^2} = -V'(u) = -\omega^2 u + \frac{u}{\sqrt{1+u^2}} \equiv f(u)\,,$$

This equation has the form $u''(x) = f(u)$. An approximate solution of an ordinary nonlinear differential equation of this form can be obtained with a Runge-Kutta scheme. We use the following "fourth-order" Runge-Kutta scheme [17].

Choose a small step-size $\Delta x$ and let the values of $x$, $u$, and $u'$ at a sequence of discrete points be denoted respectively by $x_k = k\Delta x$, $u_k = u(x_k)$, and $u'_k = u'(x_k)$, where $k$ takes on integer values. For given values at $x_j$, the next values are given by

$$u_{j+1} = u_j + [u'_j + \frac{1}{6}(k_1 + 2k_2)]\Delta x + \mathrm{O}(\Delta \mathrm{x}^4)\,,$$
$$u'_{j+1} = u'_j + \frac{1}{6}k_1 + \frac{2}{3}k_2 + \frac{1}{6}k_3\,,$$

where

$$k_1 = \Delta x f(u_j)\,,$$
$$k_2 = \Delta x f(u_j + \frac{1}{2}u'_j\Delta x + \frac{1}{8}k_1\Delta x)\,,$$
$$k_3 = \Delta x f(u_j + u'_j\Delta x + \frac{1}{2}k_2\Delta x)\,.$$

Taylor series expansions of the functions on the right-hand sides of these equations show that the error in $u_{j+1}$ is of order $\Delta x^4$. For the simulations reported here, $\Delta x$ was set equal to $0.01$, but the value $\Delta x = 0.1$ was used to obtain Fig. 8.

### 3.3 Derivation of the Equation for the Profile

Dropping the primes in Eq. (8), we consider

$$u_{tt} - u_{xx} = f(u)\,, \tag{14}$$

where $f(u)$ represents one of the restoring forces $f_j(u)$ in Eqs. (13). Substituting $u(x,t) = u(x)\cos(\omega t)$ into Eq. (14) gives

$$-\omega^2 u(x)\cos(\omega t) - u''(x)\cos(\omega t) = f[u(x)\cos(\omega t)]\,,$$

where primes denote differentiation. Multiplying both sides of this by $\cos(\omega t)$ and integrating over one period, that is, for $0 \le t \le 2\pi/\omega$, gives the nonlinear ordinary differential equation

$$u''(x) = -\omega^2 u(x) - \frac{1}{\pi}\int_0^{2\pi} f[u(x)\cos\theta]\cos\theta d\theta\,. \tag{15}$$

The variable $t$ has been eliminated.

In the integral in Eq. (15), the argument $u(x)\cos\theta$ of the first factor goes from $u(x)$ at $\theta = 0$ to $-u(x)$ $\theta = \pi$, and then back to $u(x)$ when $\theta = 2\pi$, taking on the same values in the second range as in the first. The second factor, $\cos\theta$, behaves the same way, so the integral is equal to twice the value of the integral over $0 \le \theta \le \pi$. In this range, $\cos\theta$ is odd about the midpoint value $\theta = \pi/2$, and since the function $f$ itself is odd, the integral is four times the value of the integral over the range $0 \le \theta \le \pi/2$, giving

$$u''(x) = -\omega^2 u(x) - \frac{4}{\pi}\int_0^{\pi/2} f[u(x)\cos\theta]\cos\theta\, d\theta\,.$$

The integral on the right-hand side of the last equation (including the minus sign) can be called the "nonlinear force" on the analogous mechanical particle and denoted by $f^{NL}(u)$, so we write

$$f^{NL}(u) \equiv -\frac{4}{\pi}\int_0^{\pi/2} f[u(x)\cos\theta]\cos\theta\, d\theta\,, \tag{16}$$

with which Eq. (15) now reads

$$u''(x) = -\omega^2 u(x) + f^{NL}(u)\,. \tag{17}$$

This is the equation that we solve by the Runge-Kutta method above. The integration begins at the position of the peak, taken to be $x = 0$. At $x = 0$, the amplitude is set equal to some desired value, denoted $u_{\max}$, and the derivative is set equal to 0. The method integrates to the right until the right-hand end of the string, and then we create the mirror image of this shape to extend the solution to negative values of $x$.

Equation (17) resembles Newton's Second Law, $mx''(t) = F(x)$, for a particle of unit mass in a conservative potental, as claimed, with $x$ analogous to time and $u$ analogous to the particle's position. On the left-hand side, $u''(x)$, is analogous to the acceleration $x''(t)$ in Newton's Second Law. The right-hand side is analogous to the force and is a function solely of $u$ itself, unlike dissipative friction. The total force consists of two two terms. The first term, $-\omega^2 u$, is a linear restoring force, the same as Hooke's law for a spring, and would, by itself, give the equation of motion for simple harmonic oscillation at frequency $\omega$.

The second term on the right-hand side of Eq. (17), $f^{NL}(u)$, is a nonlinear function of $u$. Since $f(u)$ is an odd function with sign opposite from that of $u$, $f^{NL}(u)$ is also odd but has the same sign as $u$. Therefore it represents a repulsive force. And since $f(u)$ saturates, $f^{NL}(u)$ also saturates. That is, when $|u| >> 1$, $f(u\cos\theta)$ becomes effectively constant, and therefore may be taken outside of the integral in Eq. (16) to leave the integral of $\cos\theta$ over a quarter-cycle, which is 1. The conclusion is that the shape of $f^{NL}(u)$ is a smoothed step-function, as shown in Fig. 9(a) below for $V_2(u)$ in Eqs. (12). Hence the linear term, on the right-hand side of Eq. (17), $-\omega^2 u$, dominates for large displacements.

We now consider the energy of the analogous particle. The energy is equal to the sum of its kinetic and potential energy and is conserved (does not vary with time). To obtain the formula for the energy, multiply each side of Eq. (17) by $u'(x)$ to obtain

$$u'(x)u''(x) = -\omega^2 u(x)u'(x) + f^{NL}[u(x)]u'(x)\,,$$

or

$$\frac{d}{dx}\frac{1}{2}[u'(x)]^2 = -\frac{d}{dx}\frac{1}{2}\omega^2 u^2(u) + f^{NL}[u(x)]u'(x)\,.$$

Using Eq. (16), we obtain

$$f^{NL}(u) = \frac{d}{du}\frac{4}{\pi}\int_0^{\pi/2} V(u\cos\theta)d\theta\,,$$

since $dV(u\cos\theta)/du = V'(u\cos\theta)\cos\theta = -f(u\cos\theta)\cos\theta$. We may define the nonlinear potential $V^{NL}(u)$ corresponding to this force with the equation

$$V^{NL}(u) \equiv -\frac{4}{\pi}\int_0^{\pi/2} V(u\cos\theta)d\theta\,, \tag{18}$$

which recovers the standard relationship between force and potential:

$$f^{NL}(u) = -\frac{d}{du}V^{NL}(u)\,. \tag{19}$$

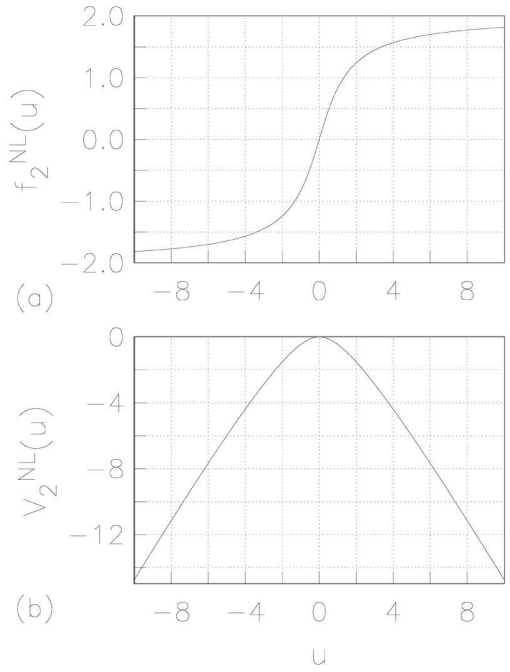


Figure 9. (a) The nonlinear force defined in Eq. (16) and (b) nonlinear potential defined in Eq. (18) for the analogous classical mechanical particle are shown for the second potential in Eqs. (12). Because $f^{NL}(u)$ is linear with positive slope for $|u| << 1$, $V^{NL}(u)$ is quadratic with negative curvature in this region.

The $\pm$ signs involved here may appear incorrect at first sight.

Note that $V^{NL}(u)$ is independent of $\omega$. Figure 9(b) shows $V^{NL}(u)$, for the second potential in Eqs. (12). Now we have, by the chain rule,

$$\begin{aligned} \frac{d}{dx}\frac{1}{2}[u'(x)]^2 &= -\frac{d}{dx}\frac{1}{2}\omega^2 u^2(x) - \frac{d}{du}V^{NL}(u)u'(x) \\ &= -\frac{d}{dx}\frac{1}{2}\omega^2 u^2 - \frac{d}{dx}V^{NL}[u(x)]\,, \end{aligned}$$

which can be integrated by inspection to obtain

$$\frac{1}{2}(u')^2 + \frac{1}{2}\omega^2 u^2 + V^{NL}(u) = E\,, \tag{20}$$

where $E$ is a constant analogous to the particle's energy. Equation (20) states that the energy of the analogous particle is conserved. The first term on the left-hand side is the kinetic energy. The other two terms are, respectively, a quadratic potential energy and a nonlinear potential energy. The curvature of the quadratic potential is $\omega^2$.

The details of the shape of $V^{NL}(u)$ in Fig. 9(b) follow from its definition in Eq. (18). If $|u| << 1$, then $V(u\cos\theta) \simeq (u\cos\theta)^2/2$, and Eq. (18) gives $V^{NL} \simeq -u^2/2$, for the integral of $\cos^2\theta$ on $0 \geq \theta \geq \pi/2$ is $\pi/4$. That is, in Eq. (18), $V^{NL} \simeq (-4/\pi)(u^2/2)\pi/4 = -u^2/2$. Hence as $|u| \to 0$, the curvature of $V^{NL} \to -1$.

From these observations, the total potential is a double well if $\omega < 1$. Figure 10 shows the sum $V^{\rm tot}$ of the two potentials for several values of $\omega$. The main point is that, as claimed, the profile of the

pseudobreather is the same as the nonperiodic trajectory of a particle with energy $E = 0$ in a double-well potential such as that in Fig. 7.

A value for $\omega$ must be known in order to integrate Eq. (17). Equation (20) provides this as a function of the amplitude. Denoting the maximum amplitude of $u(x)$, meaning its value at the turning point, by $u_{\max}$, and setting $u'(x) = E = 0$ in Eq. (20) gives us

$$\omega = \sqrt{-2V^{NL}(u_{\max})/u_{\max}^2}\,. \tag{21}$$

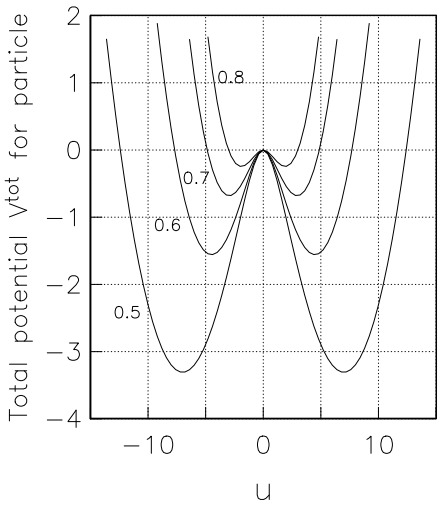


Figure 10. The sum of the linear and nonlinear potentials in Eq. (20) is shown for several values of $\omega$

The integrals in Eqs. (16) and (18) that define $f^{NL}(u)$ and $V^{NL}(u)$, respectively, are estimated by the simplest of numerical integration schemes: summing the areas of narrow rectangles. Typically 1000 rectangles were used to obtain the results reported. The results are not especially sensitive to the choice of the number of rectangles. Changes of a few percent result from using 100 or 400 rectangles instead of 1000.

The tails or wings require special handling. Small numerical errors in evaluating $\omega$ with Eq. (21) cause the particle either to get over the peak of the potential at $u = 0$ or to be reflected from it before the numerical integration reaches the end of the string, preventing it from approaching $u = 0$ asymptotically.

There are several ways to address this problem. For example, one could iterate on $u_{\max}$ or $\omega$, while holding the other fixed, until a suitable value were obtained such that the Runge-Kutta K solution decays until the end of the string is reached. The scheme we use is to halt the Runge-Kutta integration and make the tails decay exponentially as soon the logarithmic derivative $u'(x)/u(x)$ lies within $3\%$ of its limiting value at small amplitudes, namely $-\sqrt{1-\omega^2}$, which may be denoted by $-\kappa$ for brevity. Specifically, the Runge-Kutta codes tests the inequality $u'(x)/u(x) \le -0.97\kappa$. When this is satisfied, the Runge-Kutta integration is replaced by exponential decay with decay-constant $\kappa$. This is based on the following:

As noted above, Eq. (18) says that, as $u \to 0$, $V^{NL}(u) \to -u^2/2$. Equation (19) now gives $f^{NL}(u) = -dV^{NL}(u)/du = u$, and substituting this into Eq. (17) gives

$$u''(x) = (1-\omega^2)u\,.$$

This implies that $u(x)$ decays or increases exponentially with decay-constant $\kappa = \sqrt{1-\omega^2}$. That is, in the limit of small amplitude, $u(x) = u_0 \exp(\pm\kappa x)$, for some constant $u_0$. Hence, in the upper tail $u(x) = u_0 \exp(-\kappa x)$, implying that $u'(x)/u(x) = -\kappa$, as claimed above.

This page is intentionally blank.

# 4. BOOSTING

Making a breather move is called "boosting" it in the literature. To simulate a moving pseudobreather, we need to know its initial conditions, namely its shape $u(x,0)$, slope $\partial u(x,0)/\partial x$, and transverse speed $\partial u(x,t)/\partial t$ at $t=0$. We let $v$ denote the speed of the blob, with $v>0$ for motion to the right and $v<0$ for motion to the left.

For observers on a train moving at speed $v$ relative to ourselves as observers on the ground, the blob is stationary. In Section 3, we saw how to initialize a stationary pseudobreather. The initial conditions for a moving blob as seen on the ground follow from the relationship between the space and time variables on the train and ground. This involves the same transformation of space and time as that in special relativity given by a Lorentz transform (the next pair of unnumbered equations below).

The string in a trough is not itself relativistic, of course, but the properties of space and time that appear in special relativity naturally and necessarily enter into the initialization of a moving pseudobreather. The speed of waves on a free string, denoted by $c$ in Eq. (3) and given by $c=\sqrt{T/\rho}$, plays the role of the speed of light in vacuum in special relativity.

The relativistic analogy owes to the Lorentz-invariance of the operator $\partial^2/\partial t^2-\partial^2/\partial x^2$ in Eqs. (8) and (14). For our case, the pseudobreather obeys the same wave equation in different frames of reference, as in the case of light. In special relativity, no matter what their relative motion is, all frames observe that a given pulse of light has the same speed in vacuum, and as noted in Section 2.2, electromagnetic waves obey the same wave equation as that for waves on a string.

The invariance of the wave equation for the case of light follows from the Principle of Relativity: the laws of physics are the same in any frame, meaning every inertial (unaccelerated) frame of reference. The relationship between the variables for space and time in one frame and those in the other also follows from this. Special relativity derives these logically from the Principle of Relativity.

Space and time are intertwined or mixed in special relativity. We do not demonstrate that a Lorentz transform does in fact capture the four phenomena that it does, but we mention them below and give their common names (in parentheses). They are essential to understanding how a blob is reshaped when boosted. First, since the string moves in the transverse direction, its displacement is the same in both frames (invariance of distances perpendicular to the direction of motion). Second, a rod of some given length in the eyes of the train, at rest aboard the train and parallel to the tracks, is shorter in the eyes of the ground by the factor $\sqrt{1-\beta^2}\equiv 1/\gamma$ (length-contraction), where $\beta\equiv v/c$, with $c$ being the speed of light in vacuum. Third, any clock aboard the train ticks too slow in the eyes of the ground by the factor $\gamma$ (time-dilation). Fourth, the clock in the engine lags the clock in the caboose in the ground's eyes by the amount $\gamma\beta L/c$, where $L$ is the distance between caboose and engine in the ground's eyes (loss of simultaneity).

There is no loss of generality in assuming that the clocks at the origin of each frame are next to each other when each shows a time of 0. Let $x,t$ denote the position and time of an event in the ground-frame and $x',t'$ denote the position and time of this event as observed in the train-frame, the latter having speed $v$ along the positive $x$-axis. The Lorentz transform then reads

$$\begin{aligned} x' &= \gamma(x-\beta ct) \\ ct' &= \gamma(ct-\beta x)\,. \end{aligned}$$

We may set $c=1$ without loss of generality, and replace these equations by

$$\begin{aligned} x' &= \gamma(x-\beta t) \\ t' &= \gamma(t-\beta x)\,, \end{aligned}$$

These imply the following partial derivatives, to be used shortly:

$$\partial x'/\partial x = \partial t'/\partial t = \gamma\,,$$
$$\partial x'/\partial t = \partial t'/\partial x = -\gamma\beta\,.$$

In the train-frame, the pseudobreather is given by $u(x',t') = u(x')\cos(\omega t')$, the same standing-wave approximation introduced shortly after Eq. (14). We denote this using a subscript $T$ (for "train") as $u_T(x',t') = u_T(x')\cos(\omega t')$. This is to distinguish it from the symbol $u(x,t)$ representing the pseudobreather in the ground-frame.

The Runge-Kutta scheme (Sec. 3.2) is used to solve Eq. (17) in the train-frame. It yields values of $u_T(x',t'=0)$ and $\partial u_T(x',t'=0)/\partial x'$ at a set of points along the $x'$-axis. If $\Delta x$ denotes the step-size in the ground-frame, these points have spacing $\Delta x' = \gamma\Delta x$ in the train-frame, consistent with length-contraction. That is, the step-size in the ground-frame is $\Delta x = \Delta x'/\gamma$. Because transverse distances are invariant, we have

$$u(x,t) = u_T(x',t')\,.$$

On substituting the expressions for $x'$ and $t'$ in the Lorentz transform equations into this, one obtains the following expression for a boosted breather as a function of the coordinates in the ground-frame:

$$u(x,t) = u_T[\gamma(x-\beta t)]\cos[\omega\gamma(t-\beta x)]\,.$$

Setting $t=0$ gives us the initial shape of the blob in the ground-frame,

$$u(x,0) = u_T(\gamma x)\cos(\omega\gamma\beta x)\,. \tag{22}$$

On the right-hand side of this equation, the argument $\gamma x$ of $u_T$ expresses length-contraction and the argument $\omega\gamma\beta x$ of the cosine expresses the loss of simultaneity. The first factor produces a contracted bell-shaped envelope and the second factor produces symmetric spatial oscillations to the left and right of the center of the blob.

The chain-rule gives us

$$\frac{\partial u_T(x',t')}{\partial x} = \frac{\partial u_T(x',t')}{\partial x'}\frac{\partial x'}{\partial x} + \frac{\partial u_T(x',t')}{\partial t'}\frac{\partial t'}{\partial x}\,,$$
$$\frac{\partial u_T(x',t')}{\partial t} = \frac{\partial u_T(x',t')}{\partial x'}\frac{\partial x'}{\partial t} + \frac{\partial u_T(x',t')}{\partial t'}\frac{\partial t'}{\partial t}\,.$$

On substituting the above partial derivatives into these, we obtain

$$\frac{\partial u_T(x',t')}{\partial x} = \gamma\frac{\partial u_T(x',t')}{\partial x'} - \gamma\beta\frac{\partial u_T(x',t')}{\partial t'}\,,$$
$$\frac{\partial u_T(x',t')}{\partial t} = -\gamma\beta\frac{\partial u_T(x',t')}{\partial x'} + \gamma\frac{\partial u_T(x',t')}{\partial t'}\,.$$

Now $\partial u_T(x',t')/\partial x'$ is just the slope returned by the Runge-Kutta scheme times the factor $\cos(\omega t')$, and hence is equal to $u_T'(x')\cos(\omega t')$. Similarly, $\partial u_T(x',t')/\partial t'$ is just $u_T(x')$ times the derivative of $\cos(\omega t')$ with respect to $t'$, the latter of which is $-\omega\sin(\omega t')$. Making the substitutions gives

$$\frac{\partial u_T(x',t')}{\partial x} = \gamma u_T'(x')\cos(\omega t') + \gamma\beta\omega u_T(x')\sin(\omega t')\,,$$
$$\frac{\partial u_T(x',t')}{\partial t} = -\gamma\beta u_T'(x')\cos(\omega t') - \gamma\omega u_T(x')\sin(\omega t')\,.$$

Setting $t = 0$ in the Lorentz transform gives us $x' = \gamma x$ and $t' = -\gamma\beta x$. Substituting these into the last equations lets us express the initial slope and speed in terms of the spatial coordinate $x$ in the ground-frame. We can also replace $u_T(x', t')$ by $u(x, 0)$ on the left-hand side. The result is

$$\frac{\partial u(x,0)}{\partial x} = \gamma u_T'(\gamma x)\cos(\omega\gamma\beta x)) - \gamma\beta\omega u_T(\gamma x)\sin(\omega\gamma\beta x)\,, \tag{23a}$$

$$\frac{\partial u(x,0)}{\partial t} = -\gamma\beta u_T'(\gamma x)\cos(\omega\gamma\beta x) + \gamma\omega u_T(\gamma x)\sin(\omega\gamma\beta x)\,. \tag{23b}$$

Initialization was performed using these formulas along with Eq. (22) for the initial shape.

Figures 11 and 12 show four boosted blobs in the ground frame for case 3 at four speeds chosen such that $\gamma = 1, 2, 3$, and 4, with $u_{\max} = 5$ in Fig. 11 and $u_{\max} = 2$ in Fig. 12.

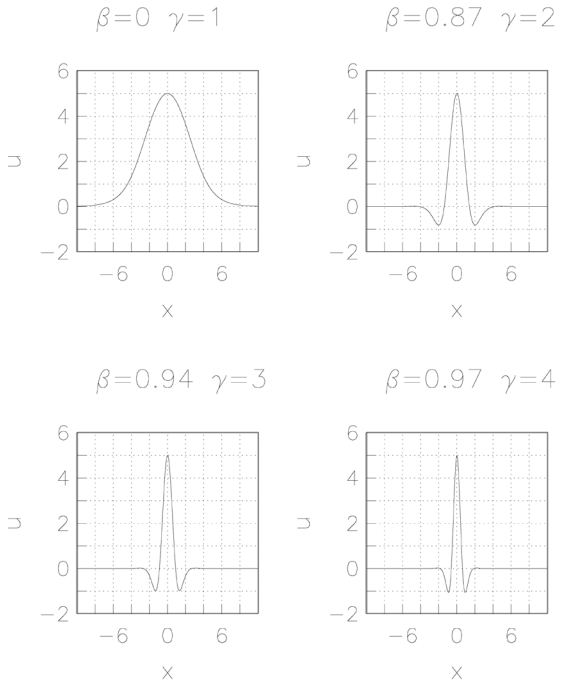


Figure 11. Four boosted blobs for case 3 are shown with amplitude 5.

The amplitude in Fig. 12, being smaller than that in Fig. 11, results in broader blobs, and hence a larger phase-difference across the body of the blob. Additional remarks on this are in Sections 6 and 7.

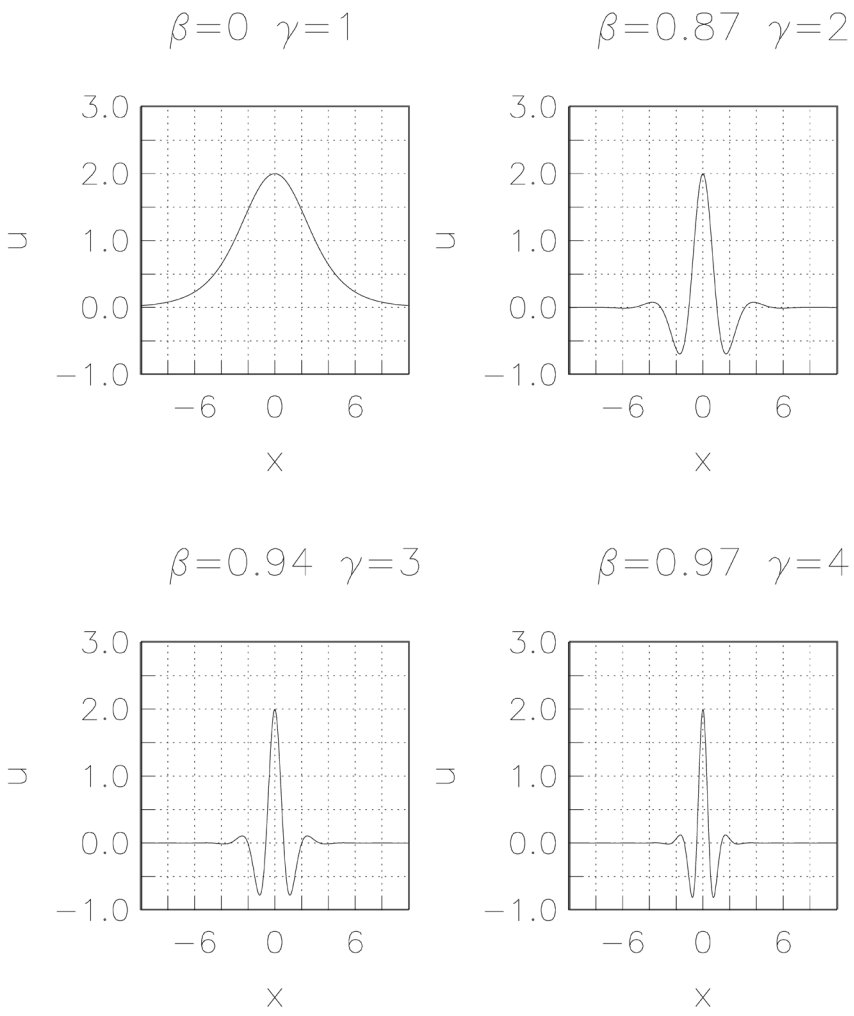


Figure 12. Four boosted blobs for case 3 are shown with amplitude 2.

# 5. FINITE-DIFFERENCE EQUATIONS

Equation (14) is solved approximately by finite-difference equations. This means we replace partial derivatives by ratios. For example, $\partial u(x,t)/\partial t$ is replaced by $[u(x,t+\Delta t)-u(x,t)]/\Delta t$ and $\partial u(x,t)/\partial x$ by $[u(x+\Delta x,t)-u(x,t)]/\Delta x$, where the space- and time-steps $\Delta x$ and $\Delta t$ are chosen to be small enough that $u(x,t)$ changes by a very small fraction in these intervals. Similar ratios replace the partial derivatives of other functions. The computations do not involve division by very small numbers, however. We will sketch the coming development, present Newton's method for completeness, develop the finite-difference equations, and finally discuss boundary conditions.

First Eq. (14) is recast as a system of three simultaneous first-order partial differential equations by defining two new functions, denoted $uf$ and $ub$, that represent, in a sense, the forward- and backward-going parts of $u(x,t)$. The partial derivatives of $uf$ and $ub$ are replaced by finite-differences on a square grid of points in the $xt$-plane, as shown in Fig. 13 below, giving a system of three simultaneous nonlinear algebraic equations for the variables at the next time-step as functions of their current values.

This system for the updated variables cannot be solved in closed form, however. But they can be obtained to high accuracy by Newton's method, iterating on a single variable and avoiding multiple matrix inversions at each time-step. Newton's method may be familiar to some readers, but is described next for completeness.

### 5.1 Newton's Method

Newton's method is a simple but efficient iterative algorithm for obtaining successively more accurate estimates of the solution of an equation of the form $F(x)=0$. Suppose that $x_0$ is an initial estimate of the value of $x$ that satisfies the equation. The next approximation is represented by $x_1=x_0+\delta x$. It is obtained by keeping only the first two terms of the Taylor series expansion of $F$ about $x_0$ and setting these equal to 0. That is, one makes the approximation

$$F(x_0+\delta x)=F(x_0)+F'(x_0)\delta x=0\,,$$

where $F'(x_0)$ denotes the derivative of $F(x)$ evaluated at $x=x_0$, which gives

$$x_1=x_0+\delta x=x_0-\frac{F(x_0)}{F'(x_0)}\,. \tag{24}$$

Repeating these steps gives the next approximation. The scheme extends a line tangent to the curve of $F(x)$ at $x=x_0$, taking the next iterate to be the value of $x$ for which this tangent intersects the $x$-axis, that is, where it vanishes. Instead of testing for convergence, we used five iterations in simulations. The scheme usually converged after only two or three with single-precision arithmetic. The first guess is always very close to the exact solution.

### 5.2 Reduction to a First-order System

Define "forward" and "backward" functions $uf(x,t)$ and $ub(x,t)$, respectively, by

$$uf = \partial u/\partial t-\partial u/\partial x\,, \tag{25a}$$
$$ub = \partial u/\partial t+\partial u/\partial x\,. \tag{25b}$$

Suppose that $u(x,t)$ is a forward-traveling wave, a fixed shape moving to the right at speed 1. Then it would depend on $x$ and $t$ in the combination $x-t$ and we could write $u=u(x-t)$. In this case, Eqs. (25) give $uf=-2u'(x-t)$ and $ub=0$, where a prime denotes differentiation with respect to the argument of a function. Similarly, if $u(x,t)$ were a backward-traveling wave with a fixed shape moving at speed 1 to the left, then it would depend on the combination $x+t$, and Eqs. (25) give $uf=0$ and $ub=2u'(x+t)$. Hence by their definition $uf$ and $ub$ extract just the forward- and backward-moving parts of $u(x,t)$ in some sense.

With $uf$ and $ub$ defined by Eqs. (25), Eq. (14) can be written as a system of three simultaneous, coupled first-order partial differential equations:

$$(\partial/\partial t+\partial/\partial x)uf=f(u)\,, \tag{26a}$$

$$(\partial/\partial t-\partial/\partial x)ub=f(u)\,, \tag{26b}$$

$$\partial u/\partial t=\frac{1}{2}(uf+ub)\,. \tag{26c}$$

As to the physical significance of $uf$ and $ub$, from basic mechanics, we know that for a string with tension $T$ and linear mass density $\rho$, the power flow $S$ in the positive $x$-direction and the energy per unit length $\rho_{\rm E}$ are given, respectively, by

$$S = -Tu_xu_t\,, \tag{27a}$$

$$\rho_{\rm E} = \frac{1}{2}\rho u_t^2+\frac{1}{2}Tu_x^2+V(u)\,, \tag{27b}$$

in which subscripts $x$ and $t$ denote partial derivatives with respect to those variables. There is no loss in generality in setting $T=\rho=1$ and regarding $x$ and $t$ as dimensionless. The inverse of Eqs. (25) reads $\partial u/\partial t=(uf+ub)/2$ and $\partial u/\partial x=(ub-uf)/2$. Substituting these into Eqs. (27) gives

$$S = \frac{1}{4}(uf^2-ub^2)\,, \tag{28a}$$

$$\rho_{\rm E} = \frac{1}{4}(uf^2+ub^2)+V(u)\,. \tag{28b}$$

These imply that $uf$ and $ub$ are, respectively and within a constant of proportionality, the densities of the momentum flowing in the forward and backward direction. The discrete version of the latter was used to compute the energy in simulations.

Equations (28) lead to the equation $\partial\rho_{\rm E}/\partial t = -\partial S/\partial x$, which is a statement of energy conservation. It says that the rate of change of the energy density at any point along the string is equal to minus the gradient of the power flow. Integrating both sides of this with respect to $x$ on the interval $a \le x \le b$, one finds that at any instant, the rate of change of the energy in this region is equal to $S(x = a, t) - S(x = b, t)$, the difference between the rate at which energy flows into this region at its left-hand end and flows out of this region at its right-hand end.

### 5.3 Finite-Difference Equations: The Method of Characteristics

The numerical scheme described below is called the "method of characteristics." It is stable, convergent, and consistent provided that $f(u)$ in Eq. (14) is differentiable [18] (meaning its slope is well defined). These properties simply mean that the algorithm is reliable. More specifically, it yields an increasingly accurate approximation to the solution of Eq. (14) as the size of the time- and space-steps is reduced. We will see that the error at each step forward in time is roughly proportional to the square of the step-size. Hence halving the step-size reduces the error by a factor of four or more.

We let $\Delta x = \Delta t = 0.01$ in simulations. The algorithm has effectively converged, since smaller step-sizes are found not to change the results significantly, nor do slighly larger step-sizes. Since $\omega < 1$, the pseudobreathers have periods $T = 2\pi/\omega > 6$, meaning that we have more than 600 time-steps per cycle. The half-width of the blobs is greater than 3 (see Fig. 15 below), so a blob is comprised of at least 600 space-steps.

The difference equations introduced below are time-centered, meaning that future and past are balanced or treated symmetrically. The algorithm works forward or backward in time with $\Delta t > 0$ or $\Delta t < 0$, respectively.

The solution is found at points in a square grid in the $xt$-plane given by $x = x_j = j\Delta x$ and $t = t_n = n\Delta t$, where $j, n$ are integers and $\Delta x = \Delta t$. Let $u$ denote the estimate of $u(x, t)$ at the point $x = j\Delta x$, $t = n\Delta t$ in the $xt$-plane with identical notation for $uf$, $ub$, and $f(u)$. In what follows, we think of $n$ as the index at the current time, at which all of the variables are known, and $n + 1$ as the index of the next time for which we seek their updated values.

To a first approximation, the partial derivative of $uf(x, t)$ with respect to $x$ evaluated at $x = (j - 1/2)\Delta x$, $t = (n + 1)\Delta t$ is

$$\left(\frac{\partial uf}{\partial x}\right)^{n+1}_{j-1/2} = \frac{uf_j^{n+1} - uf_{j-1}^{n+1}}{\Delta x}.$$

Similarly, to a first approximation, the partial derivative of $uf(x, t)$ with respect to $x$ evaluated at $x = (j - 1/2)\Delta x$, $t = n\Delta t$ is

$$\left(\frac{\partial uf}{\partial x}\right)^{n}_{j-1/2} = \frac{uf_j^{n} - uf_{j-1}^{n}}{\Delta x}.$$

The average of these expressions is the estimate of $\partial uf/\partial x$, centered at $x = (j - 1/2)\Delta x$, $t = (n + 1/2)\Delta t$, the center of the left-hand square in Fig. 13, giving

$$\left(\frac{\partial uf}{\partial x}\right)^{n+1/2}_{j-1/2} = \frac{1}{2\Delta x}(uf_j^{n+1} + uf_j^{n} - uf_{j-1}^{n+1} - uf_{j-1}^{n}).$$

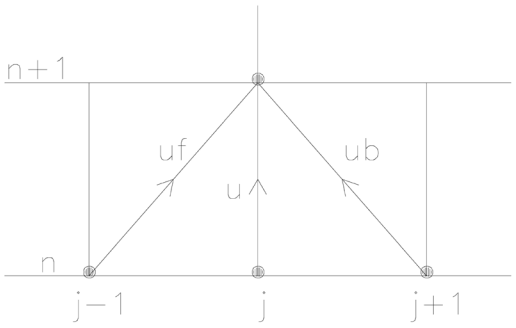


Figure 13. The space-time grid is shown to illustrate Eqs. (29) and (30). The finite-difference Eqs. (29a) and (29b) are centered at the middle of the left- and right-hand squares, respectively. Directed line segments indicate the updating of the variables next to them.

The same reasoning gives the first approximation to the partial derivative of $uf$ with respect to time centered at $x = (j - 1/2)\Delta x$, $t = (n + 1/2)\Delta t$,

$$\left(\frac{\partial uf}{\partial t}\right)_{j-1/2}^{n+1/2} = \frac{1}{2\Delta t}(uf_j^{n+1} + uf_{j-1}^{n+1} - uf_j^n - uf_{j-1}^n)\,.$$

With $\Delta x = \Delta t$, the estimate of $(\partial/\partial t + \partial/\partial x)uf$ on the right-hand side of Eq. (26a), centered at $x = (j - 1/2)\Delta x$, $t = (n + 1/2)\Delta t$ is the sum of the last two expressions. The middle two terms in each expression cancel out and the first and fourth terms are the same, leaving

$$\left[\left(\frac{\partial}{\partial t} + \frac{\partial}{\partial x}\right)uf\right]_{j-1/2}^{n+1/2} = \frac{1}{\Delta t}(uf_j^{n+1} - uf_{j-1}^n)\,.$$

This is simply the approximation of the derivative of $uf$ with respect to time along the forward characteristic from $(j - 1, n)$ to $(j, n + 1)$, as indicated by the left-hand arrow in Fig. 13. To weight past and future symmetrically, the right-hand side of Eq. (26a) is replaced by the average of $f(u)$ at each end of this line segment, which gives the finite-difference approximation

$$\frac{1}{\Delta t}(uf_j^{n+1} - uf_{j-1}^n) = \frac{1}{2}\left(f_j^{n+1} + f_{j-1}^n\right)\,.$$

The same reasoning gives the following finite-difference version of Eq. (26b) centered at $x = (j + 1/2)\Delta x$, $t = (n + 1/2)\Delta t$ (the center of the right-hand square in Fig. 13):

$$\frac{1}{\Delta t}(ub_j^{n+1} - ub_{j+1}^n) = \frac{1}{2}\left(f_j^{n+1} + f_{j+1}^n\right)\,.$$

This is the derivative taken along the backward characteristic from $(j + 1, n)$ to $(j, n + 1)$ indicated by the right-hand arrow in Fig. 13.

Rearranging the last two equations gives

$$uf_j^{n+1} = uf_{j-1}^n + \frac{\Delta t}{2}\left(f_j^{n+1} + f_{j-1}^n\right)\,, \tag{29a}$$

$$ub_j^{n+1} = ub_{j+1}^n + \frac{\Delta t}{2}\left(f_j^{n+1} + f_{j+1}^n\right)\,. \tag{29b}$$

These are the update equations for $uf$ and $ub$ at the same point, namely $(j, n + 1)$. They were obtained by centering the finite-difference equations for $uf$ and $ub$ at $(j - 1/2, n + 1/2)$ and $(j + 1/2, n + 1/2)$,

respectively. The next term on the right-hand side would be quadratic in $\Delta t$, meaning that the error varies as the square and higher powers of the step-size.

For Eq. (26c), the corresponding finite-difference equation, centered at $x = j\Delta x$, $t = (n + 1/2)\Delta t$, is obtained by equally weighting the old and new "source" terms $(uf + ub)/2$ on the right-hand side. By inspection, to a first approximation, this leads to

$$u_j^{n+1} = u_j^n + \frac{\Delta t}{4}(uf_j^{n+1} + ub_j^{n+1}) + \frac{\Delta t}{4}(uf_j^n + ub_j^n)\,. \tag{30}$$

Equations (29) and (30) are a system of three simultaneous nonlinear algebraic equations giving the updated values of $uf$, $ub$, and $u$ at the grid point $(j, n + 1)$ as functions of their old values. They can be reduced to a single update equation for $u_j^{n+1}$ by eliminating $uf_j^{n+1}$ and $ub_j^{n+1}$ using the expressions on the right-hand sides of Eqs. (29). Substituting these into Eq. (30) and rearranging terms gives

$$u_j^{n+1} - \frac{\Delta t^2}{4} f(u_j^{n+1}) - b = 0, \tag{31}$$

where

$$b = u_j^n + \frac{\Delta t}{4}(uf_{j-1}^n + uf_j^n + ub_j^n + ub_{j+1}^n) + \frac{\Delta t^2}{8}(f_{j-1}^n + f_{j+1}^n)$$

is a constant, that is, a function solely of the current values.

Equation (31) has the form $F(x) = 0$ mentioned above, with

$$F(x) = x - \frac{\Delta t^2}{4} f(x) - b$$

and hence is solvable via Newton's method. We can regard $F(x)$ as an error-function. We take the initial guess for the solution of Eq. (30), namely $u_j^{n+1}$, to be $x_0 = u_j^n$ and iterate according to Eq. (24), with

$$F'(x) = 1 - \frac{\Delta t^2}{4} f'(x)\,.$$

Hence we also need the derivatives of the forces in Eqs. (13). The expressions for these will not be displayed.

### 5.4 Boundary Conditions

To simulate decay or collisions, we do not want energy reflected from the ends of the string. We get reflectionless ends by opening up or flatten the trough near the left and right ends of the string. That is, we make the external force vanish before the ends, leaving the string free. For a free string, one can make finite-difference equations such that no energy is reflected from the ends of the string.

To achieve this, $f(u)$ is replaced by the product $a(x)f(u)$, where $a(x)$ is a so-called "boxcar" function with smoothed edges. That is, $a(x) = 1$ in a central region and falls smoothly to 0 over a certain region symmetrically about $x = 0$, the center of the string. Let $\pm x_{\max}$ denote the point at which $a(x)$ vanishes and $d$ denote the width of the transition region. That is, to the right of the origin $x = 0$, $a(x) = 1$ until $x = x_{\max} - d$ and then tapers off, reaching 0 at $x_{\max}$. To the left of the origin, $a(x)$ is the mirror image of this. We choose the weighting function $a(x)$ to use the squares of the cosine and sine, letting

$$a(x) = \begin{cases} 0 & , x \le -x_{\max} \\ \sin^2[\pi(x + x_{\max})/2d] & , -x_{\max} \le x \le -x_{\max} + d \\ 1 & , -x_{\max} + d \le x \le x_{\max} - d \\ \cos^2[\pi(x - x_{\max} + d)/2d] & , x_{\max} - d \le x \le x_{\max} \\ 0 & , x_{\max} \le x \end{cases} \tag{32}$$

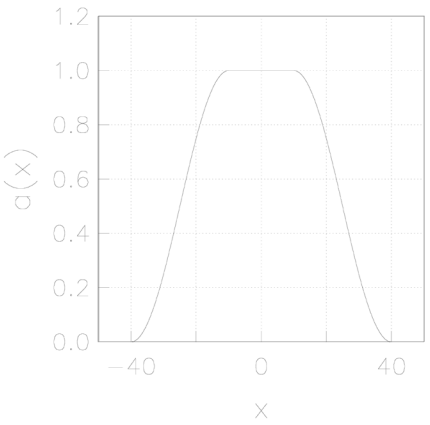


Figure 14. The trough-opening function $a(x)$ in Eq. (32) is shown for the case $x_{\max} = 40$, $d = 30$.

Figure 14 illustrates this window or weighting function for $x_{\max} = 40$, $d = 30$.

If the external force vanishes, then Eqs. (29) read

$$uf_j^{n+1} = uf_{j-1}^n \,, \tag{33a}$$
$$ub_j^{n+1} = ub_{j+1}^n \,. \tag{33b}$$

Let $J$ denote the space index at the right-hand end of the string. The string is assumed to continue indefinitely to the right past this point, but there is no source of waves to the right of the point where $j = J$. Hence we can set $ub_J^n = ub_J^{n+1} = 0$. With this and Eq. (33a), setting $j = J$ in Eq. (30) gives

$$u_J^{n+1} = u_J^n + \frac{\Delta t}{4}(uf_{J-1}^n + uf_J^n) \,.$$

At the left-hand end of the string, the mirror image of the above applies. We have $uf_1^n = uf_1^{n+1} = 0$, since there is no source of waves to the left of the point where $j = 1$. With this and Eq. (33b), setting $j = 1$ in Eq. (30) gives

$$u_1^{n+1} = u_1^n + \frac{\Delta t}{4}(ub_2^n + ub_1^n) \,.$$

From the above, the complete set of update equations at the ends of the string are as follows: At the left end,

$$uf_1^{n+1} = 0 \,, \tag{34a}$$
$$ub_1^{n+1} = ub_2^n \,, \tag{34b}$$
$$u_1^{n+1} = u_1^n + \frac{\Delta t}{4}(ub_2^n + ub_1^n) \,, \tag{34c}$$

and at the right end,

$$uf_J^{n+1} = uf_{J-1}^n \,, \tag{35a}$$
$$ub_1^{n+1} = 0 \,, \tag{35b}$$
$$u_J^{n+1} = u_J^n + \frac{\Delta t}{4}(uf_{J-1}^n + uf_J^n) \,. \tag{35c}$$

# 6. SIMULATIONS

This section first discusses the width of the pseudobreathers, then their decay over many cycles, their absorption by nearly reflectionless boundaries, and finally collisions between moving and stationary pseudobreathers.

### 6.1 Widths

Strictly speaking, the topic of widths does not fall under simulations but initialization. We discuss the widths of pseudobreathers here in part to avoid lengthening Section 3 on initialization and in part because initialization is the first stage of simulation.

The initial width of a pseudobreather can be defined as its half-width-at-half-maximum (HWHM) and for each case depends on the amplitude $u_{\max}$. For each case in Eqs. (12), the HWHM turns out to have a minumum value of roughly 3 when $u_{\max}$ is somewhere in the range of roughly 2-10. Figure 15 shows the HWHM for cases 1, 2, and 6 as functions of $u_{\max}$.

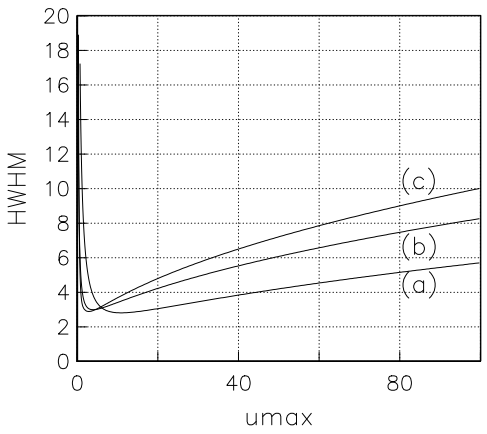


Figure 15. The HWHM is shown as a function of the maximum amplitude for (a) case 1, (b) case 2, and (c) case 6 in Eqs. (12).

### 6.2 Decay

Figure 16 shows, for each case, a plot of the energy vs. time. In each case, $u_{\max} = 4$ and the simulation was for $5000$ cycles. The percentage of energy lost is shown in each subplot. Figure 17 shows the same data but plots the natural logarithm of the energy. It appears that the pulses decay exponentially for the most part. The different behavior for case 4 may result from a coding error or from a loss of precision in computations. Case 4 requires the most involved calculations of the force per unit length and its derivative.

Figure 18 shows, for each case, a plot of the percentage of energy lost vs. $u_{\max}$ over $1005$ cycles for each integral value of $u_{\max}$. The plots only extend far enough to make the behavior clear. In case 1, probably the loss is so small that it cannot be calculated accurately in single-precision arithmetic. That is, the energy gain reflects numerical error. It also should be mentioned in addition that the energy fluctuates, owing to random numerical error, from step to step by a fraction of roughly $1 \times 10^{-6}$.

### 6.3 Absorption

Figure 19 shows a boosted pseudobreather initially centered at $x = -20$ being absorbed at the right-hand boundary for case 1 with $\beta = 0.8$ and $u_{\max} = 4$. The energy loss exceeds $99.99\%$. The near

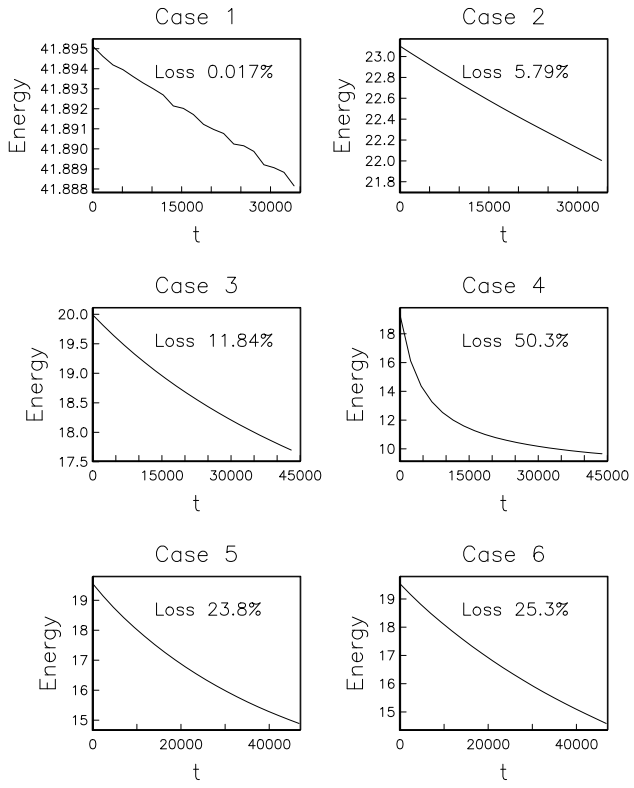


Figure 16. The energy is shown vs. time for $5000$ cycles using $u_{\max} = 4$.

total absorption means that studies of decay of pseudobreathers are not significantly affected by energy reflected from the boundaries.

### 6.4 Collisions

Figures 20 and 21 both show six collisions between an "incident" (moving) and a "target" (stationary) pseudobreather, each with amplitude of 5 for case 3 in Eqs. (12) and (13). In each figure, the incident blob has speed $0.8$. In each figure, the collisions differ only in the initial position of the incident blob. Figures 20 and 21 differ in the initial location of the target, which is $x = 10$ in Fig. 20 and is $x = 20$ in Fig. 21. The figures each show 21 snapshots of the string over a time interval of 200.

Since the snapshots are at time-intervals of 10, there is significant "aliasing" or "strobing." The lower part of Fig. 6 shows that the period of the target blob is about $10$. Hence the subfigures do not show the individual cycles of either blob. Each is sampled roughly once per cycle.

One might think that in the center-of-mass frame, the collisions shown in Figs. 21 and 20 would be symmetric, meaning invariant under reflection about the origin $x = 0$, because the blobs have equal amplitudes and the amplitude of a blob is Lorentz-invariant. If the collision were symmetric in the center-of-mass frame, there would be no excuse for either blob to alter its speed, so the figures might seem incorrect based on symmetry. This is not the case, however, since the blobs are not mirror images in the center-of-mass frame because their phases are not mirror images. A collision that is symmetric in the

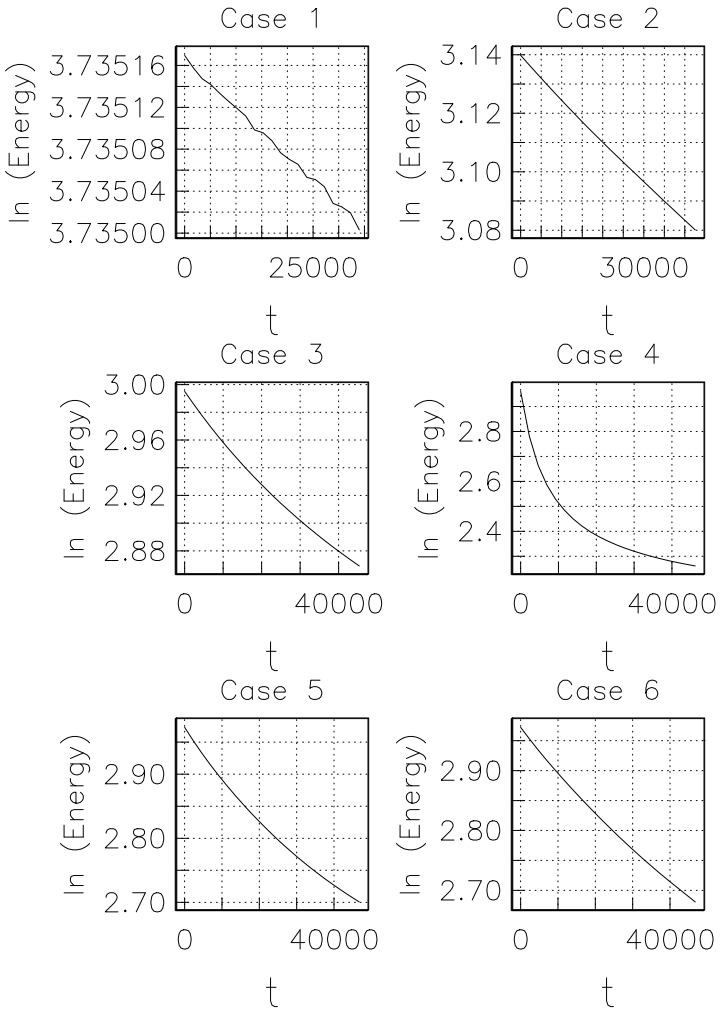


Figure 17. For the same cases as in Fig. 16, the natural logarithm of the energy is shown vs. time for $5000$ cycles for $u_{\max} = 4$.

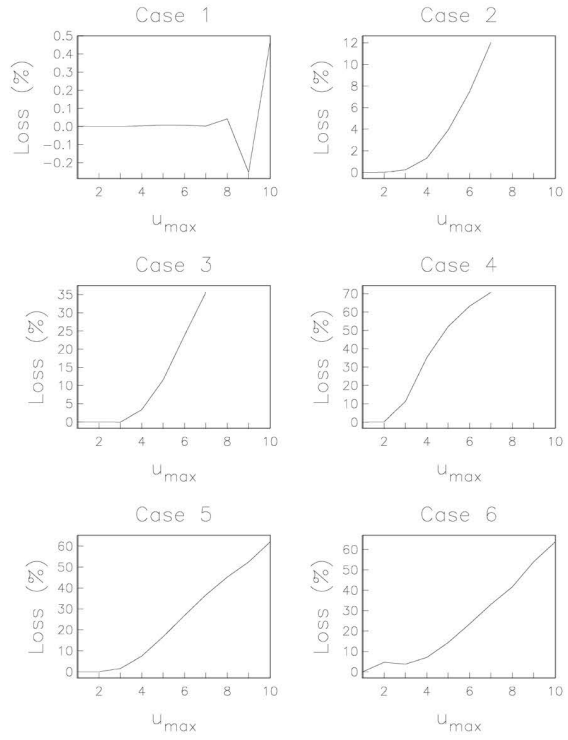


Figure 18. The percentage of energy lost is shown vs. $u_{\max}$ over $1005$ cycles.

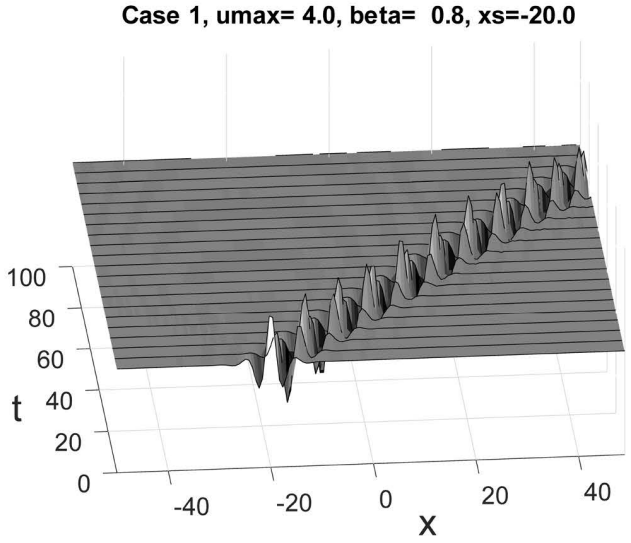


Figure 19. A surface plot is shown for a boosted breather for case 1. The amplitude is $4$ and speed $0.8$. The loss of energy exceeds $99.99\%$.

center-of-mass frame must be set up carefully in the laboratory frame to take into account the synchronized phases of the blobs in the center-of-mass frame.

To rephrase this, one might expect that in a collision between two blobs of equal amplitude, they would emerge from the collision with their speeds unchanged. It is true that if the initial conditions were symmetric in the center-of-mass frame, then the collision would have to be symmetric as well. Also, since

the wave equation is second-order in time, a collision would look the same whether it were seen running forward or backward in time. One might therefore expect the blobs to retain their initial speeds after the collision. This is not what Figs. 20 and 21 show.

The main feature that these figures show is that moving blobs can be either attracted to or repelled from each other. As mentioned, we have no theory for this effect.

Several kinds of collisions (not shown) have been simulated different from those in Figs. 20 and 21 and show a similar effect. For example, in sets of collisions between an incident and target blob in which the amplitude of the incident blob changes by $0.1$ from collision to collision, the same alternating attraction and repulsion was observed.

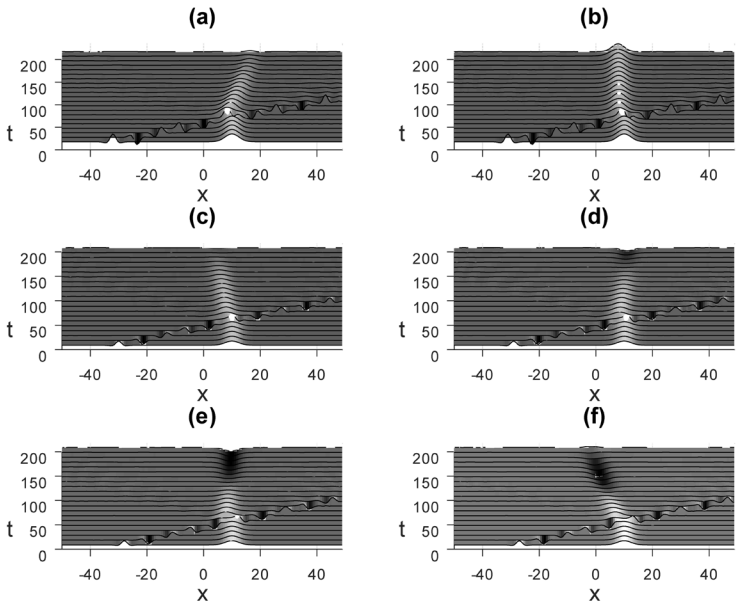


Figure 20. Collisions are shown for case 3 in which both blobs have amplitude $5$, the incident blob has speed $0.8$, and the target blob is at $x = 10$ initially. The incident blob is initially at $x = -32, -31, \ldots, -27$ in part (a), (b), ..., (f), respectively.

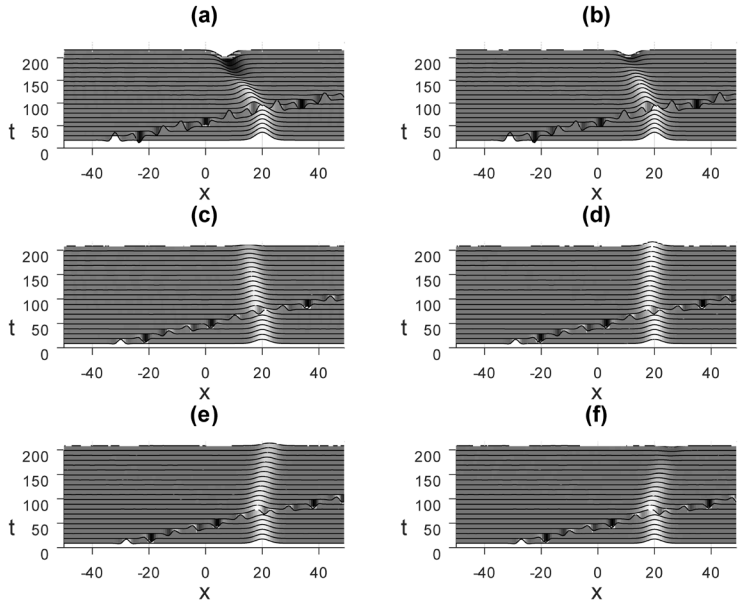


Figure 21. Collisions are shown for case 3 in which both blobs have amplitude $5$, the incident blob has speed $0.8$, and the target blob is at $x = 20$ initially. The incident blob is initially at $x = -32, -31, \ldots, -27$ in part (a), (b), ..., (f), respectively.

# 7. CONCLUDING REMARKS

It was mentioned in the Executive Summary and early in Section 1 that breatherlike waves on graphene nanotubes might ultimately advance technology beyond today's semiconductor devices. Research aimed at developing nanoscale graphene electronic devices has, in fact, seen intensive activity for over a decade. Graphene offers a reduction in size, relative to silicon technology, of roughly a factor of ten. Most work in this area seems to concern the electronic properties of nanotubes or graphene generally, however, as opposed to the mechanical, electromechanical, and magnetostatic phenomena discussed in this report.

The difference between the fourth, fifth, and sixth potentials in Eqs. (12) is almost imperceptible in Fig. 4. Similarly, the fourth, fifth, and sixth forces in Fig. 5 appear to be the same. In Fig. 6, however, one can see a difference in frequency and period between the fourth, fifth, and sixth cases. It was not by intent or design that the last three cases lie so close to each other.

Most of the potential energy functions in Eqs. (12) and corresponding forces in Eqs. (13) were found by trial and error. They do not follow any particular pattern. Indeed, efforts to construct functions with the desired properties in an orderly, systematic sequence using only ratios of polynomials failed. In retrospect, this probably relates to the fundamental theorem of algebra. This states that a polynomial of degree $n$ has $n$ roots. Higher-degree polynomials therefore have more and more wiggles. They cannot be suppressed by taking their ratios.

Two criteria drove the selection of the functions in Eqs. (12) and (13). One was that both functions be expressible either algebraically or with standard function subroutines that can be called in Fortran. Another was that the forces should approach their asymptotic limits monotonically. This turns out to be necessary for the blobs to be long lived. It was found that if a force overshoots its limiting asymptotic value, then the blobs satisfying the corresponding KG equation decay relatively rapidly, depending on their amplitude.

If the force approaches its asymptotic value monotonically, then the resonant frequency obviously decreases monotonically with increasing amplitude. This ensures that the small-amplitude wings do not radiate, as discussed in Section 2.4. A local overshoot in some range of $u_{\max}$ would increase the frequency of a blob in this range, which should reduce its self-trapping, although its frequency would still be smaller than the cut-off frequency.

The wave equation of interest, Eq. (14), as noted above, is linear for small displacement, since each potential $V_j(u)$ $(1 \le j \le 6)$ in Eqs. (12) obeys $V_j(u) \to u^2/2$ as $u \to 0$, giving $f_j(u) \to -u$. We chose potentials so that $V_j(u) \to A|u|$ as $|u| \to \infty$, for some positive constant $A$. Hence, for large amplitudes, the restoring force is a constant or "saturates," as shown in Fig. 5. This means Eq. (14) is a nonlinear wave equation at large displacement, but the nonlinearily can be removed trivially. A linear potential and the resulting constant force means that the string is in free-fall. The trough on its own produces a constant acceleration along the length of the string. In free-fall with acceleration $g$, a body has height

$$h(t) = h(0) + v_0 t - \frac{1}{2} g t^2,$$

for some constants $h(0)$ and $v_0$. This motion can be subtracted from $u(x,t)$ to remove it and leave us with the equation for a free string, with the only force arising from the string's curvature.

Alternatively, we know that being in free-fall is to be weightless, like astronauts on the International Space Station. One is unaware of the acceleration. It cannot be detected. Therefore the string behaves in this accelerating frame like a free string. It is weightless but still has mass and inertia. The conclusion is that a string obeying a saturably nonlinear KG equation like those studied here is therefore almost linear. It is tightly confined in the degree to which it can behave nonlinearly. This is quantified in the particular case of Forni's solution, which has only about $0.14\%$ of its energy in the harmonics.

It was claimed in Section 1 that Forni's solution cannot be simulated. This is because the external restoring force is discontinuous. As noted in Section 5.3, the method of characteristics requires the force to be differentiable. At the point of discontinuity at the bottom of a V-shaped trough, the force is not differentiable. Alternatively, Section 5.1 says that the derivative of the force is needed to use Newton's method. It could not be used if the derivative of the force were undefined or discontinuous.

Using independent approaches, both Forni and the author attempted to simulate Forni's breather shortly after it was found. We do not go into the details of these simulations, but the author's blobs quickly developed spikes and decayed, while collisions simulated by Forni showed that the blobs did not retain their initial shapes to high accuracy.

We have not discussed in detail how the author's pseudobreathers relate to other breathers. We only noted that the breatherlike blobs in the overdense region of a relativistic plasma seen in the author's thesis [13] are closely related to plasma cavitons. The literature on breathers is extensive. Hundreds of papers or conference proceedings have treated plasma cavitons alone and breathers have been studied in several saturable media. As noted, apparently there has been no prior systematic study of breatherlike entities that arise in saturable KG equations.

The study of breathers has seen roughly comparable activity along experimental, numerical, and theoretical lines. Breathers have been investigated, one way or another, in nanotubes, hydrodynamic systems, nonrelativistic and relativistic plasmas, DNA, Josephson junctions, spin-waves, Bose-Einstein condensates (superconductors), micromechanical oscillators, and magnetic metamaterials (materials not occurring naturally). Several new breathers have been reported in recent years. One might guess that breathers ultimately will prove more interesting than solitons.

It has been suggested that a movie of colliding pseudobreathers be made. This would be time-consuming and it is not clear whether the effort would be rewarded by deeper insight into the nature of pseudobreathers' decay or collisions. The time-lapse figures in Section 6 would seem to let one inspect the details of a collision better than a movie since the pulses hold still for the eye. The question nevertheless remains interesting.

None of Eqs. (2), (3), (4), nor (14) describe a string in a trough under the force of gravity as claimed. A string in a trough was introduced to provide a concrete, intuitive picture and not because the saturable KG equations here describe such a system exactly. This is because a string confined to the wall of a trough moves both horizontally and vertically, whereas our equations ignore vertical motion.

One could, however, minimize the importance of the vertical motion of a string in a trough to any desired degree. One could make the slope of the walls sufficiently small. Such a flattening of the trough would not affect our results, as the trough could retain the features responsible for the properties of the blobs, namely a parabolic bottom and walls that become linear asymptotically.

A ball in a parabolic bowl is similar. Its potential energy is a quadratic function of its displacement in the horizontal direction, but it does not oscillate sinusoidally since it moves in both the horizontal and vertical direction. In contrast, a ball attached to a spring obeying Hooke's law that moves only vertically or horizontally does oscillate sinusoidally, at least to a first approximation.

As mentioned, the string in Fig. 1 moves only in one direction. Hence it obeys the KG equation for the second restoring force in Eqs. (13). The system in Fig. 1 could also be replaced by its replica using the force of gravity, since the electric field of a point charge is given by the same equation as the gravitational field of a point-mass, within a constant of proportionality.

A uniformly positively charged string that vibrates in the midplane between two fixed, parallel strings (parallel to them and perpendicular to their plane) with uniform negative charge density also obeys a saturable KG equation [14], namely

$$u_{tt} - u_{xx} = -\omega^2 \frac{u}{1+u^2} \,,$$

in dimensionless variables and for a certain constant $\omega$, for which the corresponding potential per unit length is

$$V(u) = \frac{1}{2}\omega^2 \ln(1+u^2) \,.$$

The derivation is left to the reader, but we note that this potential has a seagull-wing shape in contrast to the V-shaped troughs in Eqs. (12). We omit discussion of pseudobreathers for seagull-wing shaped potentials to avoid lengthening this report.

There is another case in which the string obeys the above KG equation. In the system of three charged strings just mentioned, each string could be replaced by a wire carrying a constant current. With the current in each wire flowing in the same direction, the resulting magnetostatic force would equal the electrostatic force in the system of three charged strings within a constant of proportionality. The reason is that the magnitude of the magnetic field $\mathbf{B}$ that loops around a straight wire carrying a steady current is proportional to the reciprocal of the distance from the wire, and hence falls off like the magnitude of the electric field of a uniformly charged line. In this latter example, the Lorentz force on the flexible wire is in the same direction as the electrostatic force on the flexible charged wire in the former case.

Regarding the pseudobreathers' widths, they approach $\infty$ as the amplitude $u_{\max}$ approaches zero and $\infty$. The width may be defined as the half-width at half-maximum for present aims. It decreases rapidly as $u_{\max}$ increases from $0$ until reaching a minimum. As the amplitude increases past this point, the width increases slowly, eventually growing roughly as the square root of $u_{\max}$, as is the case for Forni's breather [15]. The minimum widths lie in the range from about $3$ to $5$ and occur for $u_{\max}$ in the range from about $2$ to $3$, roughly where each potential has become effectively linear. The KdV and sine-Gordon breathers are different, becoming narrower with increasing amplitude. Beyond this, we do not compare the width of other breathers with that of ours.

We turn to the question of why boosted blobs have the shapes they have. We should be able to explain these shapes. In Section 4, Eq. (22), we saw that the initial shape of a boosted pseudrobreather is

$$u(x,0) = u_T(\gamma x)\cos(\omega\gamma\beta x)\ ,$$

the product of a bell-shaped curve and a modulating cosine. The first factor is a contracted replica of a stationary pseudobreather in its own frame, which we called the train-frame. The phase of the second factor, $\omega\gamma\beta x$, arises from the loss of synchronization between the caboose and engine clock. Does the phase in the second factor lead to an ever-increasing number of ripples in the envelope of a boosted pseudobreather as its speed nears the speed of waves on a free string?

It does not, on the following grounds. In the limit of large speed, $\beta \simeq 1$, so the arguments of the two functions are nearly equal within a constant of proportionality. In its own frame, a pseudobreather has some width we may call $d$. We need not be precise, and $d$ may be taken to be the half-width at half-maximum, the full-width at half-maximum, or any other measure. This implies that, over the main body of the blob, phase is roughly $\omega\gamma x \simeq d$. Hence in the ground's eyes, the phase difference in radians across the main body of a boosted pseudobreather is equal to the width of the pseudobreather in its own frame, within a constant of proportionality, however defined. This width is not a function of its speed in the ground's eyes. Therefore the phase difference across the main body of the breather does not grow arbitrarily large as the blob is boosted to nearly the speed of waves on a free string.

It should be pointed out that the phase difference is not necessarily small, however. We saw that for each trough, the width of a blob has a minimum as a function of its amplitude $u_{\max}$ and increases without bound as the amplitude $u_{\max}$ approaches 0 or $\infty$. This behavior is seen in the initialized blobs.

It was mentioned at the end of Section 1 that KG equations are almost the simplest form of wave equation. The form of the simplest wave equation is

$$\partial u/\partial t - v\partial u/\partial x = 0\ ,$$

called a hyperbolic equation [1]. The symbol $v$ may be a constant or a function of $u$ itself, not to mention other possibilities, so this equation may describe nonlinear waves.

Breathers in discrete systems have drawn much interest in recent years. The system is a lattice of connected point-masses rather than a continuous medium. One major subject in this area is the stability of discrete breathers. A new language has developed to describe discrete systems that includes the terms "on-site" and "off-site" potentials.

Interest in discrete systems is not at all new. In the mid-50s, Fermi, Pasta, and Ulam (FPU), with thermodynamics in mind, simulated coupled nonlinear springs in a famous study that presaged the solution of the KdV equation [19]. Their intent was to observe the thermalization of an initial vibration owing to nonlinear springs in an idealized model of a crystal. It was subsequently shown that the KdV equation is the continuum limit of the spring-mass problem studied by FPU.

Numerical studies have led the way several times in physics. Lorenz's 1963 weather simulations of air flow provided early insight into chaos theory [20] in showing exponential sensitivity to initial conditions. Most of us have heard some variant of, "A butterfly flapping its wings in Brazil, ..." In 1965, Zabusky and Kruskal, in effect, observed KdV solitons in simulations of plasma waves [21], preceding and motivating the two-year search that ultimately yielded the IST. They noted the same striking and unexpected phenomenon seen by FPU: the near recurrence of the initial conditions.

Another case was Feigenbaum's 1979 numerical study (using a hand-held calculator) of the so-called "logistic" equation. This work revealed the period-doubling route to chaos [22]. It explained for the first time the way that a rudder periodically sheds vortices. In the so-called von Karmen vortex-street behind a tiller, the period of shedding doubles at specific Reynolds numbers on its way to fully developed turbulence. The difference between the critical period-doubling values of the Reynolds numbers gets smaller and smaller until the point at which the period becomes infinite. Feigenbaum's work showed that this same pattern emerged in the approach to chaos in his studies of the logistic equation.

Nonlinear wave theory might be likened to lasers in their early years: a solution looking for a problem. Solitons have seen at least one practical application, however. Their use in fiber optic communications reduces the need for repeaters that reconstruct the original waveforms. It is unclear how widespread this practice is, however.

A nonlinear optical phenomenon called "degenerate four-wave mixing" may find practical application as well. This involves three intersecting laser beams in a Kerr medium (in which the change in the index of refraction is proportional to the intensity), two being strong counterpropagating "pump" beams and a third and weaker one called the "probe" beam propagating at right angles to the pump beams. The nonlinear combination of three waves creates a fourth beam which counterpropagates to the probe and is the "phase-conjugate" version of the probe beam. On traveling backward through the medium that caused wavefront abberations on the probe beam, the phase-conjugate beam's aberrations are removed.

Aside from practical applications, physics satisfies our curiosity about nature. In this connection, solitons may play a role in neural signaling, specifically in initiating the firing of action potentials in the outer layers of a neuron. There was speculation, now likely dropped, that the arms of spiral galaxies arise not from rotation, but instead from nonlinear gravitational interactions among gas or stars. It has also been suggested that Jupiter's giant red spot might be a soliton. A considerable literature appears to show that rogue waves are breathers.

The numerical results here provide a partial answer for a fundamental question in nonlinear wave theory: How nearly can nonintegrable wave equations, meaning ones without an IST, yield pseudobreathers that mimic true breathers? The most interesting question arising from this work is how one can analyze the exchange of momentum in the collision of pseudobreathers.

This page is intentionally blank.

# REFERENCES


1. Whitham, G. B. 1974. *Linear and Nonlinear Waves*, John Wiley & Sons, Inc.

2. Resnick, R. and Halliday, D. 1965. *Physics for Students of Science and Engineering*, John Wiley & Sons, Inc., 4th ed.

3. Marburger, J. H. 1975. "Self-focusing: Theory," *Prog. Quantum Electron.*, vol. 4, pp. 35–110, in which self-focusing in saturable Kerr media is discussed on pp. 46-48 and 67-70.

4. Russell, J. S. 1845. "Report on Waves," Tech. rep., British Association for the Advancement of Science, York, September 1844.

5. Emmerson, G. S. 1977. *John Scott Russell: A Great Victorian Engineer and Naval Architect*, John Murray.

6. Boussinesq, J. 1877. "*Essai sur la theorie des eaus courantes*," *l'Acad. des Sci. Inst. Nat. France*, vol. XXII, pp. 1–680.

7. Korteweg, D. J. and de Vries, G. 1895. "On the Change of Form of Long Waves Advancing in a Rectangular Canal, and on a New Type of Long Stationary Waves," *Philosophical Magazine*, vol. 39, pp. 422–443.

8. Gardner, C. S., Greene, J. M., Kruskal, M. D., and Miura, R. M. 1967. "Method for solving the Korteweg-deVries equation," *Phys. Rev. Lett.*, vol. 19, p. 1095.

9. Novikov, S., Manakov, S. V., Pitaevski, L. P., and Zakharov, V. E. 1984. *Theory of Solitons: The Inverse Scattering Method*, Consultants Bureau, a Division of Plenum Publishing Corporation.

10. Zakharov, V. E. and Shabat, A. B. 1972. "Exact Theory of Two-Dimensional Self-focusing and One-dimensional Self-modulation of Waves in Nonlinear Media," *Soviet Journal of Experimental and Theoretical Physics*, vol. 34, pp. 62–69, orig. Zh. Eksp. Teor. Fiz. vol. 61, 1971, 118.

11. Ablowitz, M. J., Kaup, D. J., Newell, A. C., and Segur, H. 1973. "Method for Solving the Sine-Gordon Equation," *Phys. Rev. Lett.*, vol. 30, p. 1262.

12. Kruskal, M. D. 1974. "The Korteweg-deVries Equation and Related Evolution Equations, Nonlinear Wave Motion," *Lectures in Appl. Math.*, vol. 15, pp. 61–83.

13. Shockley, R. C. 1977. *Theory of inhomogeneous self-focusing and pulse reflection in a relativistic plasma*, Ph.D. thesis, University of Southern California.

14. Shockley, R. C. 1987. "Self-trapped states in a saturable Klein-Gordon equation," *Phys. Rev. A*, vol. 35, pp. 4729–4737.

15. Forni, R. J. and Shockley, R. C. 2018. "Simplest breather," *Phys. Rev. E*, vol. 97, p. 052210–1.

16. Dwight, H. B. 1961. *Tables of Integrals and Other Mathematical Data*, The Macmillan Company, 4th ed., **48.18, 48.13**.

17. Abramowitz, M. and Stegun, I. A. 1964. *Handbook of Mathematical Functions*, National Bureau of Standard, ninth printing, 1970, **25.5.22**.

18. Courant, R., Isaacson, E., and Rees, M. 1952. “On the Solution of Nonlinear Hyperbolic Differential Equations by Finite Differences,” *Comm. Pure and Appl. Math.*, vol. 5, pp. 243 – 255.

19. Fermi, E., Pasta, J., and Ulam, S. 1974. “Studies of Nonlinear Problems, I,” *Lectures in Applied Mathematics*, vol. 15, p. 143, Science laboratory report no. la-1940 (1955), University of Chicago Press, 2:978, 1965.

20. Lorenz, N. E. 1963. “Deterministic nonperiod flow,” *J. Atmos. Sci.*, vol. 20, p. 130.

21. Zabusky, N. J. and Kruskal, M. D. 1965. “Interactions of ‘Solitons’ in a Collisionless Plasma and the Recurrence of Initial States,” *Phys. Rev. Lett.*, vol. 15, p. 240.

22. Feigenbaum, M. J. 1979. “The Universal Metric Properties of Nonlinear Transformations,” *J. Stat. Phys.*, vol. 21, pp. 669–706.

# INITIAL DISTRIBUTION

| | | |
|---|---|---|
| 84310 | Technical Library/Archives | (1) |
| 56490 | T. L Jones | (1) |

Defense Technical Information Center
Fort Belvoir, VA 22060–6218 (1)

This page is intentionally blank.

# REPORT DOCUMENTATION PAGE

*Form Approved*
*OMB No. 0704-01-0188*



**PLEASE DO NOT RETURN YOUR FORM TO THE ABOVE ADDRESS.**

| 1. REPORT DATE *(DD-MM-YYYY)* | 2. REPORT TYPE | 3. DATES COVERED *(From - To)* |
|---|---|---|
| May 2022 | Final | |

**4. TITLE AND SUBTITLE**

Pseudobreathers in Saturable Klein-Gordon Equations.

**5a. CONTRACT NUMBER**

**5b. GRANT NUMBER**

**5c. PROGRAM ELEMENT NUMBER**

**6. AUTHORS**

Richard C. Shockley
**NIWC Pacific**

**5d. PROJECT NUMBER**

**5e. TASK NUMBER**

**5f. WORK UNIT NUMBER**

**7. PERFORMING ORGANIZATION NAME(S) AND ADDRESS(ES)**

NIWC Pacific
53560 Hull Street
San Diego, CA 92152–5001

**8. PERFORMING ORGANIZATION REPORT NUMBER**

TR-3275

**9. SPONSORING/MONITORING AGENCY NAME(S) AND ADDRESS(ES)**

The NIWC Pacific Naval Innovative Science and Engineering Program
53560 Hull Street
San Diego, CA 92152–5001

**10. SPONSOR/MONITOR'S ACRONYM(S)**

NISE

**11. SPONSOR/MONITOR'S REPORT NUMBER(S)**

**12. DISTRIBUTION/AVAILABILITY STATEMENT**

DISTRIBUTION STATEMENT A:
Approved for public release. Distribution is unlimited.

**13. SUPPLEMENTARY NOTES**

This report was written by Richard C. Shockley who has retired. Tomas L. Jones is acting as key contact for this report listed in box 19a.

**14. ABSTRACT**

The first objective of the work reported here was to determine, by numerical simulations, whether self-localized, nonlinear waves akin to "breathers" exist for a certain subset of "saturable" Klein-Gordon (KG) equations. (Terms are explained in Section 1.) Breatherlike waves do arise in these equations, so the second objective was to study their decay and their interaction in collisions. Saturable KG equations govern diverse physical systems. The simplest example is a taut string subject to an external restoring force transverse to its length at rest. This could be the force of gravity on a string sliding on the wall of a V-shaped trough with a rounded, parabolic bottom. The restoring force is proportional to the displacement for small displacements from equilibrium and monotonically approaches a constant value asymptotically, or "saturates," for large displacements.

**15. SUBJECT TERMS**

Pseudobreathers; saturable Klein-Gordon equations; nonlinear waves

| 16. SECURITY CLASSIFICATION OF: | | | 17. LIMITATION OF ABSTRACT | 18. NUMBER OF PAGES | 19a. NAME OF RESPONSIBLE PERSON |
|---|---|---|---|---|---|
| a. REPORT | b. ABSTRACT | c. THIS PAGE | | | Thomas L. Jones |
| U | U | U | SAR | 62 | 19B. TELEPHONE NUMBER *(Include area code)* 619-553-7092 |

This page is intentionally blank.

This page is intentionally blank.

DISTRIBUTION STATEMENT A:
Approved for public release. Distribution is unlimited.


Naval Information Warfare Center Pacific (NIWC Pacific)
San Diego, CA 92152-5001